

CHAPTER 8

EFFECT OF SEMIRIGIDITY OF JOINT ON SEISMIC PERFORMANCE OF RC PLANE FRAMES

8.1 NEED FOR INCORPORATING SEMIRIGID JOINTS

From the literature review presented in Chapter 3, it can be seen that a lot of research has been done to study the effect of rigidity of the joint on the seismic performance of a building frame. It has been undoubtedly stated that the rigidity of the beam to column joint affects the seismic performance. Although, a lot of research has been done on the behavior of steel frames, in the modern day scenario of fast construction with precast concrete members, the rigidity of the beam column joint calls for a critical investigation. It was pointed out by some of the researchers that as the rigidity of the beam to column joint decreases from fully rigid to pinned, the fix end moment due to lateral loads shows a peculiar behavior. This fact prompted for a mathematical model to be constructed and to be analyzed under varying joint stiffness when subjected to lateral loads.

8.2 EXAMPLE FOR VARIFICATION OF MODELING ASPECTS

To study the effects of joint flexibility on the moments developed at the end of beams due to lateral loads, a plane frame model of a steel structure was studied by Ahmed and Ahmad [53]. The frame was supported at three points and vertical force and moment at the supports developed due to fully rigid connections and semi rigid connections were compared. The same model which is shown in **Fig. 8.1**, is created here on SAP2000 with the given properties. The base reactions are calculated and compared using a frame with i) fully rigid joints and ii) all joints with a rigidity of 59.33×10^5 kNm/rad.



The moments due to lateral loads and vertical loads are plotted at the encircled end of the top storey of the frame shown in **Fig. 8.1**, for the same model using a range of joint rigidity from zero (pinned) to fully rigid. Variation of moment with joint rigidity is depicted in tabular format in **Table 8.2** and in a graphical form in **Fig. 8.2**.

Table 8.2 Moments at Encircled End due to Varying Joint Rigidity

Joint Stiffness in kNm/rad	Earthquake load moment kNm	Live load moment kNm
0	0	0
100	19.47	1.00
200	34.72	1.99
1000	87.59	9.60
2000	99.55	18.55
5000	89.23	41.85
10000	69.58	71.99
15000	58.19	94.62
20000	51.14	112.15
50000	35.53	166.63
100000	29.26	196.40
250000	25.11	217.96
650000	23.30	225.50
1221500	23.61	227.10
2000000	22.56	229.27
2443000	22.50	229.50
3000000	22.44	229.76
3664500	22.41	229.92
4000000	22.37	230.01
Fully Rigid	22.34	230.14

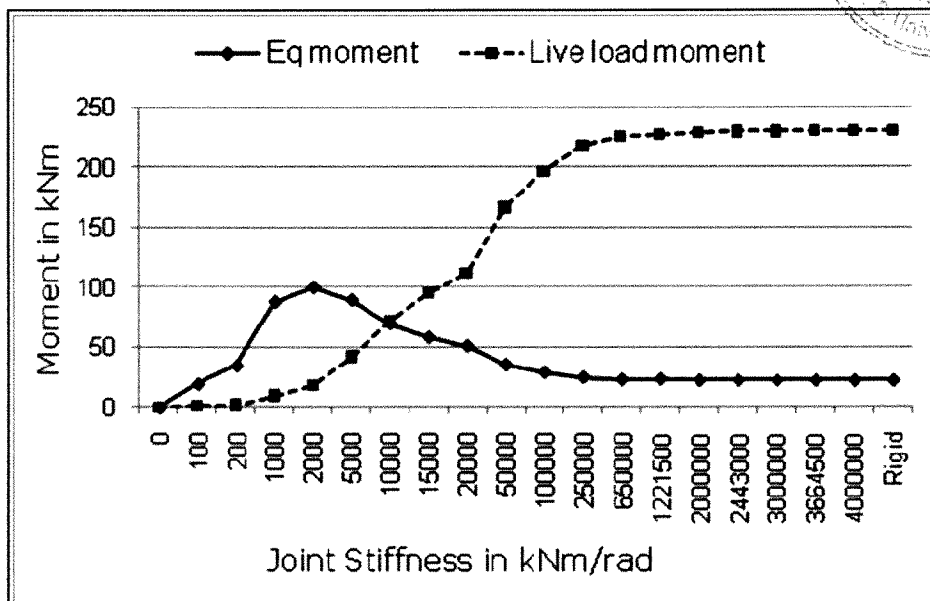


Fig. 8.2 Variation of Moment as a Function of Joint Stiffness

It is observed from the graph of **Fig. 8.2** that as the stiffness of the joints increases, the value of moment at the encircled end at roof level for live load case increases monotonically. As against this, the moment at the same end for earthquake forces, initially increases, reaches a peak value and then decreases with increase in stiffness of the joint. It is also observed that the peak value of moment which is 99.55 kNm is almost **4.45** times the value of moment (22.34 kNm) if all the joints are considered fully rigid under the same lateral load. This phenomenon is observed for lateral loads only, which is clear from **Fig. 8.2**. It is seen that live load moments do not show this behavior.

8.3 EFFECT OF SEMIRIGIDITY ON BEAM MOMENTS

The effect of semi rigidity of the joint for an RC plane frame is studied more in details by considering 1 bay 1 storey frame to 2 bay 8 storey frames with an increment of a storey and a bay. In all, 8 mathematical models having single bay and 8 models having two bays are studied. The

moments at left end of each beam, marked A, B, C, etc. as shown in **Fig. 8.3** under lateral load is noted for each of these frames for a variation in joint stiffness. For the two bay frame, moments are noted at A and a, B and b, etc. which corresponds to the left end of each beam on each storey. The geometry considered consists of bay width of 3m and a storey height of 4m for all models.

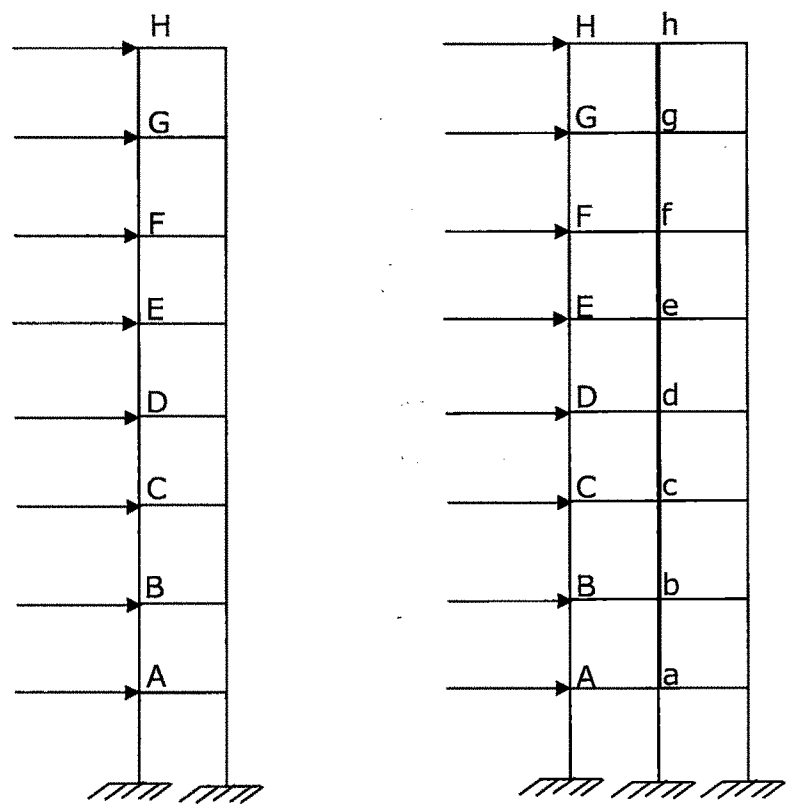


Fig. 8.3 Plane Frames considered for Analysis with Semi Rigid Joints

The cross section of all frame members is considered as 230mm x 450mm. The gravity loads in the form of uniformly distributed load on beams is given as DL = 21.5 kN/m, LL = 4 kN/m for terrace floor and DL = 23.8 kN/m, LL = 4 kN/m on typical floor is considered. Earthquake loads are applied at each storey level as per IS 1893, 2002 provisions. The results for moments developed due to earthquake load for each of the

rigidities of the beam ends is tabulated and plotted on a graph. They are presented as **Table 8.3** thru **Table 8.8** for single bay frames and representative **Tables 8.9** and **8.10** for 2 bay frames. Each of the tables shows the peak value by a shaded cell and the corresponding rigidity of the joint is noted. The variation in moment due to variation in joint rigidity is plotted as **Fig. 8.4** thru **8.11** for single bay frames and as **Fig. 8.12** thru **8.19** for 2 bay frames. In all, the trend of variation in the moment developed in the beams due to variation in the rigidity is thoroughly studied for a range of plane frame structures having one and two bays. The plot of moments developed at the end of beams on all the stories with varying rigidity is included on the same graph to represent the trend.

Table 8.3 Earthquake Moments for 1, 2 and 3 Storey Frames

Joint Stiffness	1 Storey	2-Storey		3-Storey		
	A	B	A	C	B	A
0	0	0	0	0	0	0
100	0.42	1.38	1.06	2.77	2.53	1.66
200	0.83	2.69	2.08	5.77	4.84	3.19
1000	3.84	11.16	8.89	19.01	18.14	12.47
2000	7.01	18.32	15.13	27.89	27.77	19.94
3000	9.68	23.24	19.84	32.74	33.86	25.19
5000	13.91	29.44	26.62	37.42	41.30	32.51
6000	15.61	31.47	29.18	38.58	43.79	35.25
7000	17.11	33.07	31.39	39.34	45.79	37.59
10000	20.69	36.23	36.52	40.32	50.06	43.07
20000	27.36	39.96	46.06	39.85	56.68	53.26
30000	30.65	40.86	51.00	38.77	59.54	58.48
50000	33.92	44.76	51.63	37.24	62.19	63.88
60000	34.84	41.09	57.8	36.73	62.91	65.57
75000	35.83	40.99	59.51	36.15	63.66	67.18
100000	36.86	40.81	61.37	35.51	64.43	69.02
Fully rigid	40.37	39.66	68.23	33.05	66.93	87.68

Table 8.4 Earthquake Moments for a 4 Storey Frame

Joint Stiffness	4-Storey Frame			
	D	C	B	A
0	0	0	0	0
100	4.51	4.33	3.63	2.21
200	8.36	8.08	6.82	4.19
1000	25.94	26.16	23.20	14.96
2000	34.35	36.31	33.82	22.84
3000	37.84	41.69	40.38	28.26
5000	40.04	47.25	48.53	35.75
6000	40.22	48.88	51.33	38.56
7000	40.16	50.10	53.62	40.97
10000	39.37	52.45	58.61	46.55
20000	36.36	55.47	66.59	56.77
30000	34.42	56.56	70.02	61.87
50000	32.31	57.50	73.10	67.05
60000	31.68	57.75	73.92	68.55
75000	31.00	58.00	74.75	70.16
100000	30.27	58.27	75.59	71.89
Fully rigid	27.72	59.19	78.11	77.95

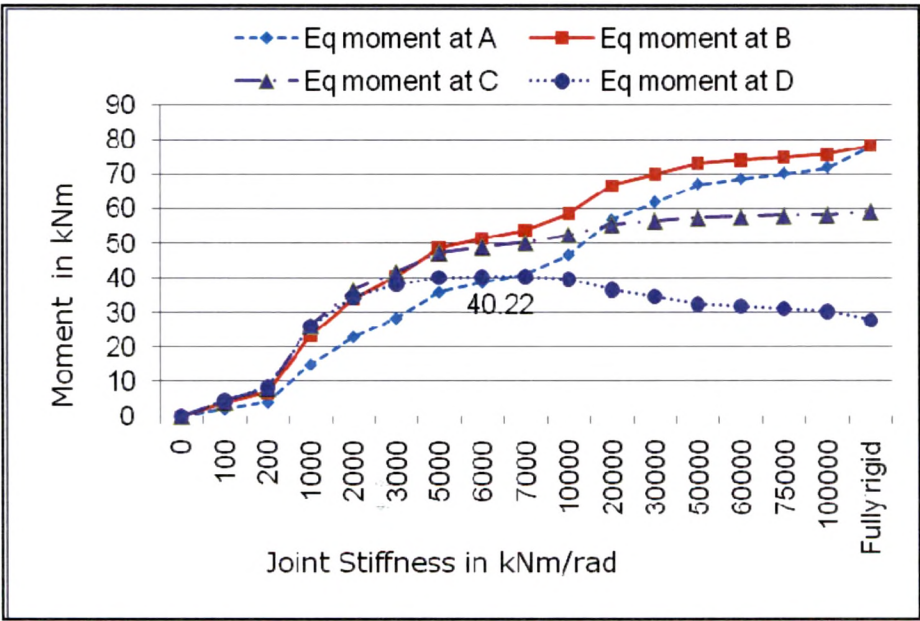


Fig. 8.4 Variation of Earthquake Moment for a 4 Storey Frame

Table 8.5 Earthquake Moments for a 5 Storey Frame

Joint Stiffness	5-Storey Frame				
	E	D	C	B	A
0	0	0	0	0	0
100	6.54	6.42	5.86	4.67	2.73
200	11.75	11.6	10.67	8.57	5.06
1000	31.37	32.41	31.54	26.78	16.7
2000	38.05	41.32	42.44	37.83	24.73
3000	39.86	45.2	48.37	44.67	30.22
5000	39.78	48.44	55.01	53.28	37.81
6000	39.23	49.21	57.1	56.25	40.64
7000	38.59	49.73	58.75	58.69	43.05
10000	36.71	50.54	62.13	63.95	48.61
20000	32.53	51.23	66.91	72.13	58.6
30000	30.34	51.41	68.74	75.49	63.54
50000	28.15	51.59	70.27	78.41	68.48
60000	27.52	51.65	70.66	79.16	69.91
75000	26.86	51.72	71.05	79.91	71.45
100000	26.16	51.81	71.44	80.66	73.1
Fully rigid	23.76	52.19	72.59	82.81	78.9

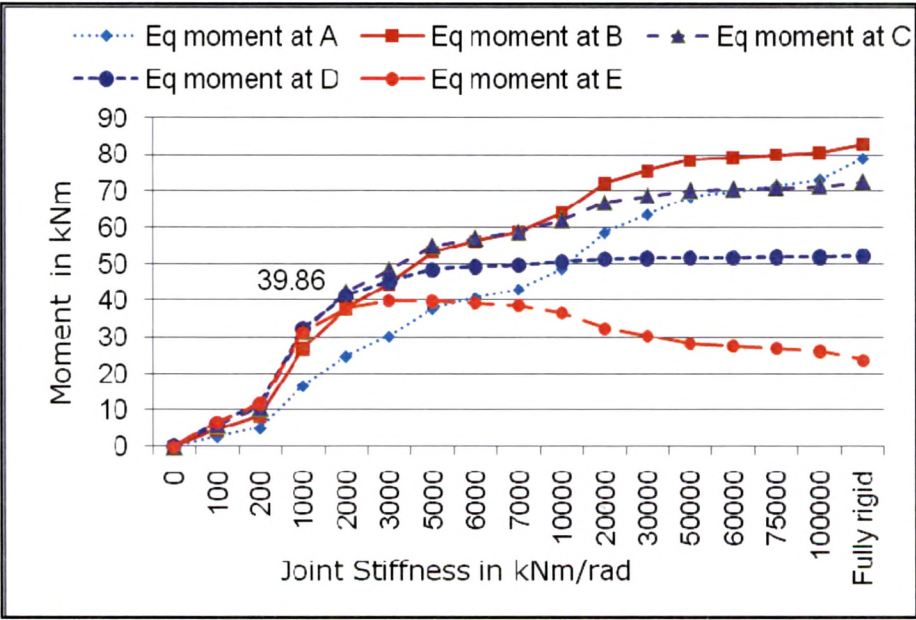


Fig. 8.5 Variation of Earthquake Moment for a 5 Storey Frame

Table 8.6 Earthquake Moments for a 6 Storey Frame

Joint Stiffness	6-Storey Frame					
	F	E	D	C	B	A
0	0	0	0	0	0	0
100	8.8	8.72	8.28	7.29	5.63	3.21
200	15.25	15.22	14.58	12.97	10.11	5.82
1000	35.25	36.89	37.59	35.52	29.36	17.95
2000	39.73	43.79	47.23	46.96	40.68	26.06
3000	39.98	46.07	51.85	53.38	47.71	31.59
5000	38.19	47.31	56.48	60.76	56.56	39.2
6000	37.15	47.43	57.83	63.12	59.59	42.02
7000	36.17	47.44	58.85	64.99	62.05	44.41
10000	33.71	47.42	60.84	68.77	67.31	49.89
20000	29.12	46.68	63.45	73.96	75.26	59.62
30000	26.94	46.45	64.42	75.81	78.43	64.39
50000	24.83	46.32	65.26	77.28	81.13	69.2
60000	24.24	46.3	65.47	77.64	81.81	70.6
75000	23.61	46.3	65.7	77.98	82.49	72.09
100000	22.96	46.31	65.93	78.32	83.17	73.7
Fully rigid	20.76	46.47	66.66	79.23	85.08	79.36

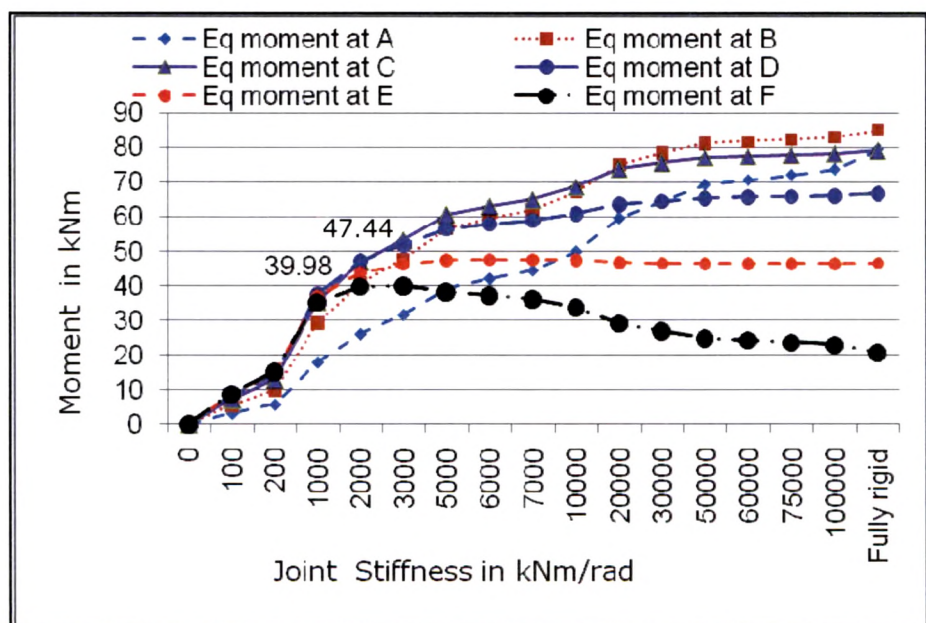


Fig. 8.6 Variation of Earthquake Moment for a 6 Storey Frame

Table 8.7 Earthquake Moments for a 7 Storey Frame

Joint Stiffness	7-Storey Frame						
	G	F	E	D	C	B	A
0	0	0	0	0	0	0	0
100	11.19	11.15	10.02	10.02	8.61	6.51	3.65
200	18.7	18.77	18.39	17.21	14.95	11.42	6.48
1000	37.78	39.85	41.68	41.65	38.53	31.28	18.87
2000	40.04	44.53	49.42	52.02	50.39	42.77	27.03
3000	39.04	45.41	52.83	57.31	57.14	49.92	32.58
5000	36.06	45.14	55.46	62.9	64.91	58.83	40.15
6000	34.74	44.82	56.21	64.58	67.37	61.84	42.93
7000	33.57	44.51	56.77	65.86	69.29	64.27	45.29
10000	30.87	43.74	57.8	68.35	73.13	69.41	50.68
20000	28.24	42.53	59.17	71.51	78.17	77.04	60.17
30000	24.15	42.12	59.72	72.58	79.88	80.04	64.84
50000	22.17	41.86	60.24	73.42	81.18	82.58	69.56
60000	21.62	41.81	60.39	73.63	81.48	83.22	70.93
75000	21.04	41.77	60.54	73.83	81.77	83.85	72.4
100000	20.44	41.74	60.7	74.03	82.05	84.48	73.98
Fully rigid	18.42	41.79	61.25	74.62	82.77	86.24	79.56

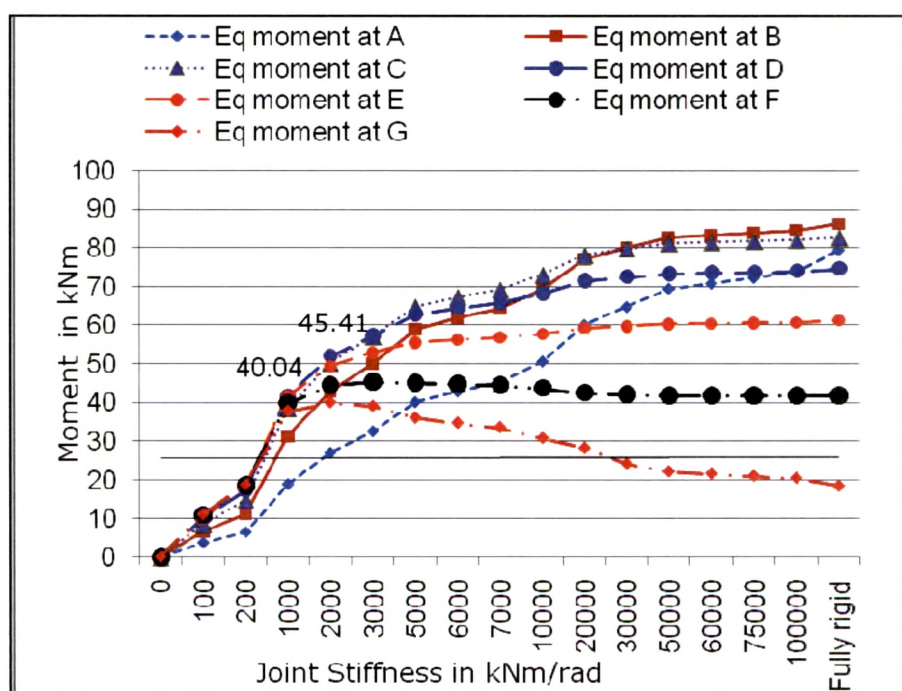


Fig. 8.7 Variation of Earthquake Moment for a 7 Storey Frame

Table 8.8 Earthquake Moments for a 8 Storey Frame

Joint Stiffness	8-Storey							
	H	G	F	E	D	C	B	A
0	0	0	0	0	0	0	0	0
100	13.35	13.35	13.14	12.53	11.40	9.64	7.18	3.98
200	21.49	21.65	21.53	20.76	19.12	16.36	12.34	6.92
1000	38.26	40.60	43.30	44.85	44.14	32.32	19.33	23.91
2000	38.40	43.05	48.85	53.39	55.01	52.33	43.83	27.45
3000	36.40	42.75	50.73	57.36	60.71	59.22	50.97	32.94
5000	32.66	41.36	52.11	61.25	66.77	67.05	59.75	40.39
6000	31.20	40.75	52.42	62.35	68.56	69.49	62.69	43.11
7000	29.96	40.23	52.65	63.18	69.92	71.36	65.05	45.41
10000	27.20	39.11	53.06	64.75	72.51	75.10	70.02	50.64
20000	22.74	37.55	53.70	66.73	75.61	79.84	77.32	59.91
30000	20.78	37.03	54.02	67.43	76.60	81.41	80.18	64.47
50000	18.96	36.66	54.37	68.01	77.33	82.56	82.59	69.09
60000	18.46	36.59	54.48	68.16	77.49	82.82	83.20	70.44
75000	17.94	36.52	54.59	68.31	77.66	83.08	83.80	71.88
100000	17.39	36.46	54.71	68.46	77.82	83.31	84.40	73.43
Fully rigid	15.57	36.39	55.13	68.92	78.26	83.91	86.06	78.92

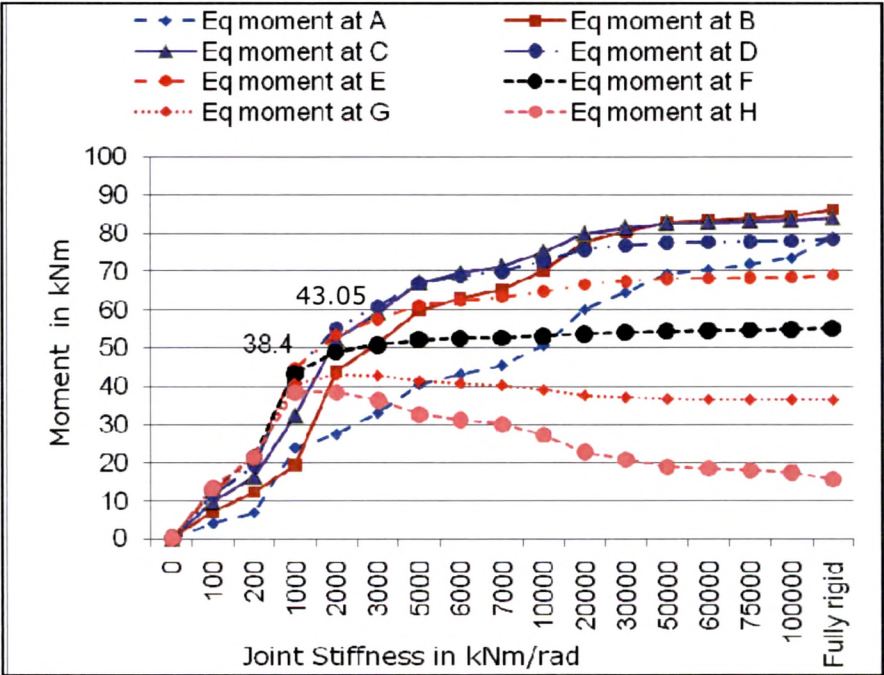


Fig. 8.8 Variation of Earthquake Moment for a 8 Storey Frame

Table 8.9 Earthquake Moments for a 1 Storey 2 Bay Frame

Joint Stiffness	1-Storey 2-Bay Frame	
	A	a
0	0	0
100	0.05	0.047
200	0.09	0.094
1000	0.42	0.41
2000	0.75	0.7
3000	1.01	0.91
5000	1.39	1.18
6000	1.54	1.27
7000	1.66	1.33
10000	1.95	1.43
20000	2.43	1.38
30000	2.65	1.2
50000	2.88	0.85
60000	2.95	0.71
75000	3.03	0.53
100000	3.12	-0.315
Fully rigid	3.52	-0.83

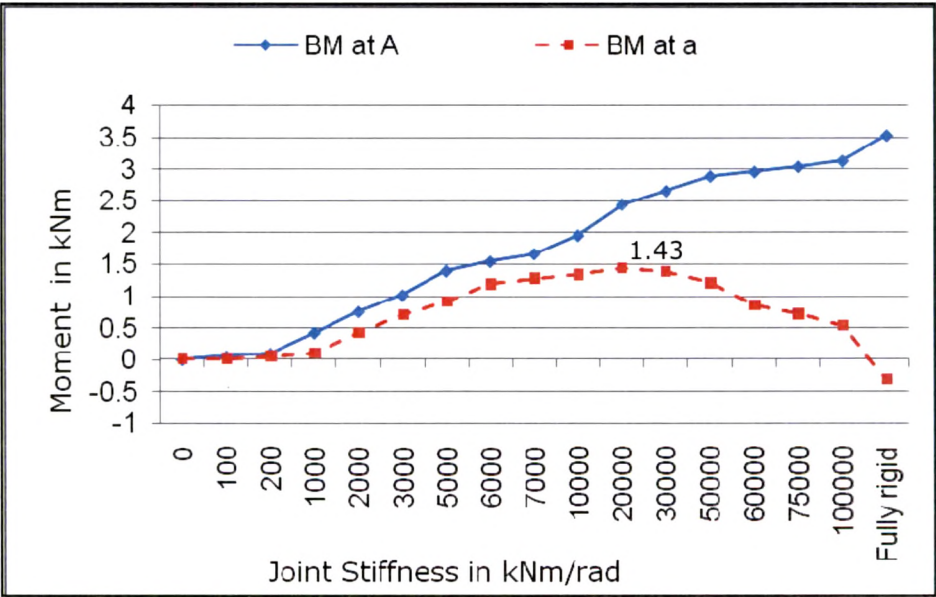


Fig. 8.9 Variation of EQ. Moment for a 1 Storey 2 Bay Frame

Table 8.10 Earthquake Moments for a 2 Storey 2 Bay Frame

Joint Stiffness	2-Storey 2-Bay Frame			
	B	b	A	a
0	0	0	0	0
100	1.84	1.84	1.42	1.42
200	3.57	3.55	2.76	2.76
1000	14.14	13.84	11.37	11.30
2000	22.4	21.56	18.79	18.57
3000	27.76	26.32	24.19	23.76
5000	34.18	31.62	31.79	30.85
6000	36.21	33.17	34.64	33.43
7000	37.78	34.29	37.08	35.59
10000	40.82	36.25	42.78	40.45
20000	44.34	37.71	53.46	48.77
30000	45.21	37.56	59.05	52.64
50000	45.54	36.96	65.00	56.47
60000	45.54	36.77	66.79	57.48
75000	45.49	36.40	68.73	58.61
100000	45.39	36.03	70.85	59.79
Fully rigid	44.64	34.43	78.62	63.76

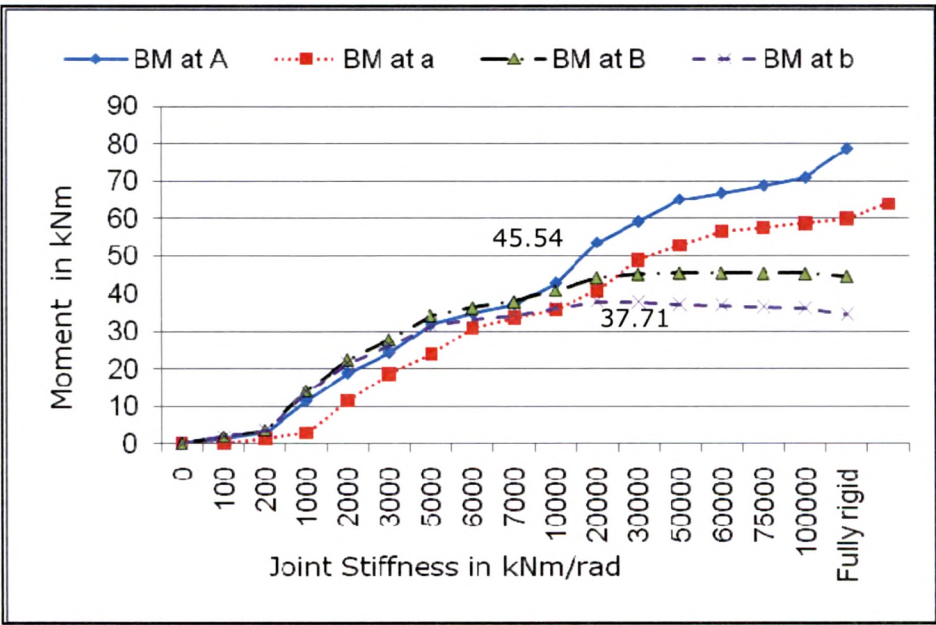


Fig. 8.10 Variation of EQ. Moment for a 2 Storey 2 bay Frame

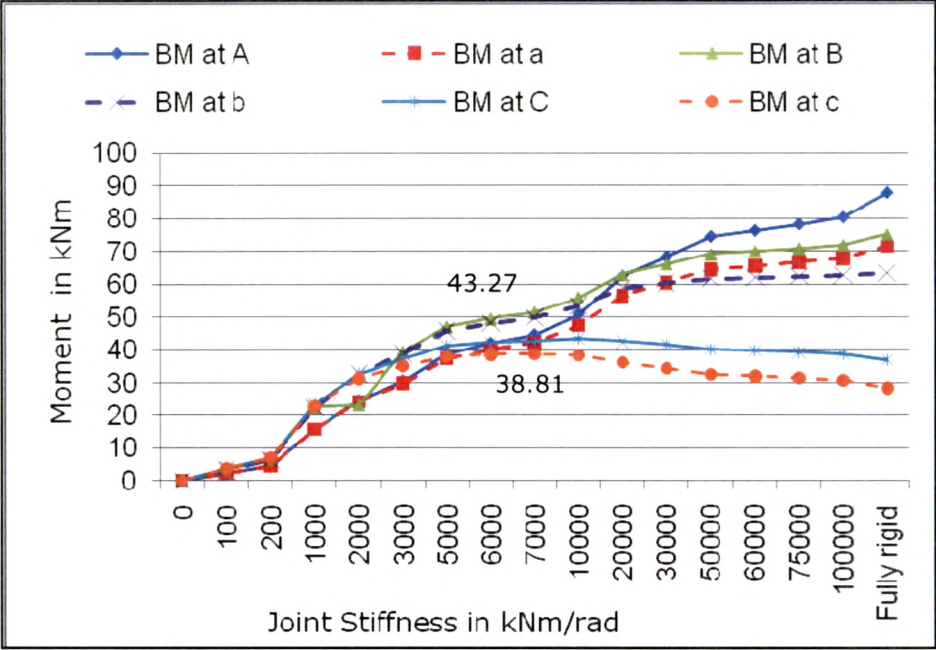


Fig. 8.11 Variation of EQ. Moment for a 3 Storey 2 Bay Frame

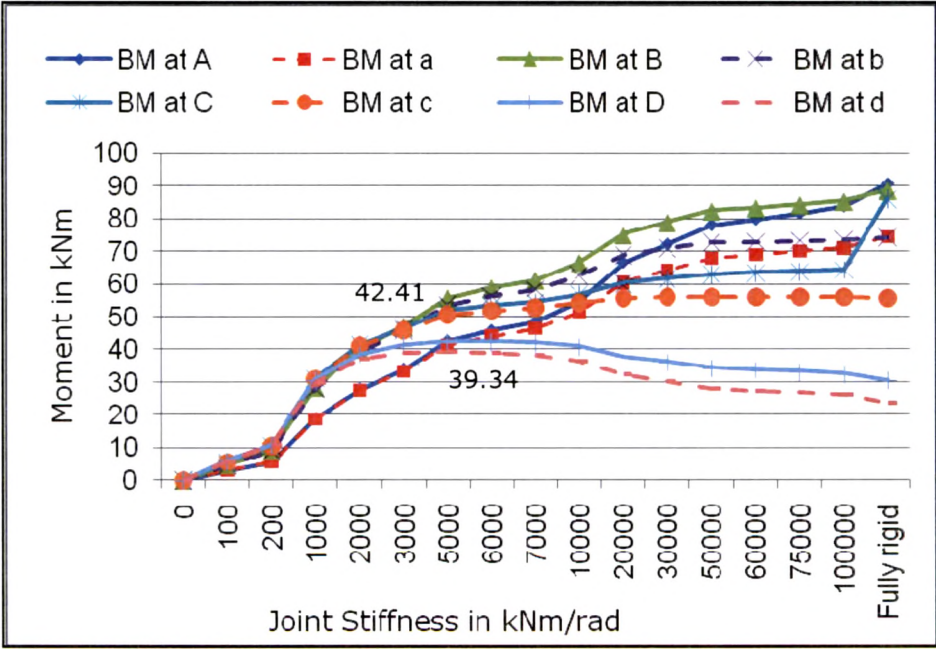


Fig. 8.12 Variation of EQ. Moment for a 4 Storey 2 Bay Frame

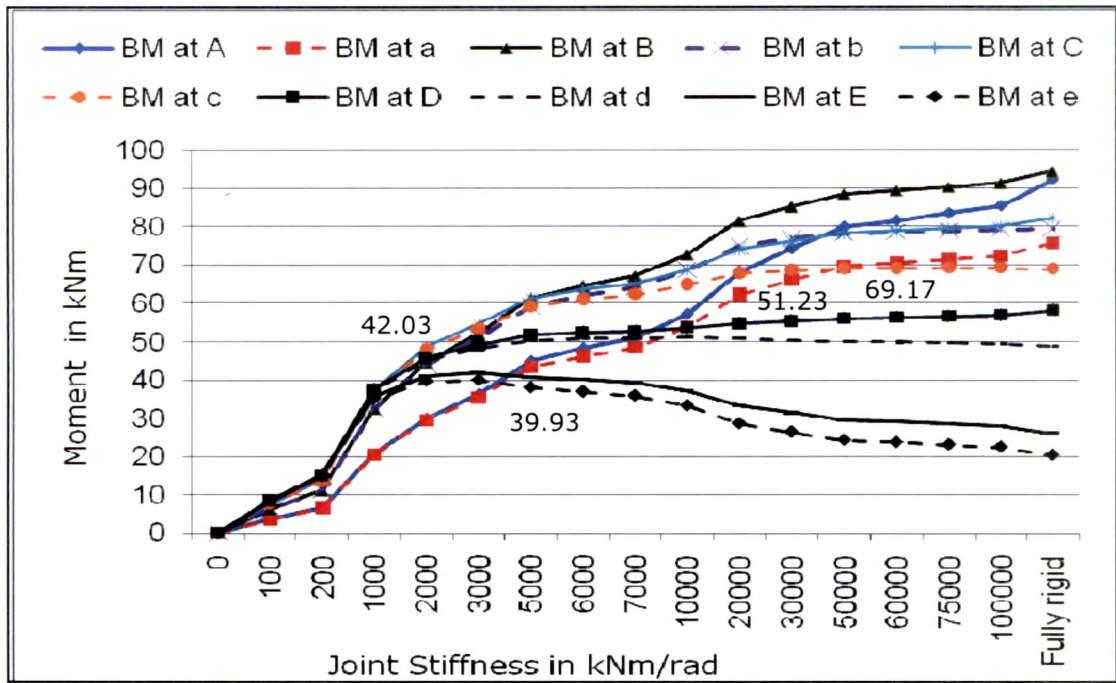


Fig. 8.13 Variation of EQ. Moment for a 5 Storey 2 bay Frame

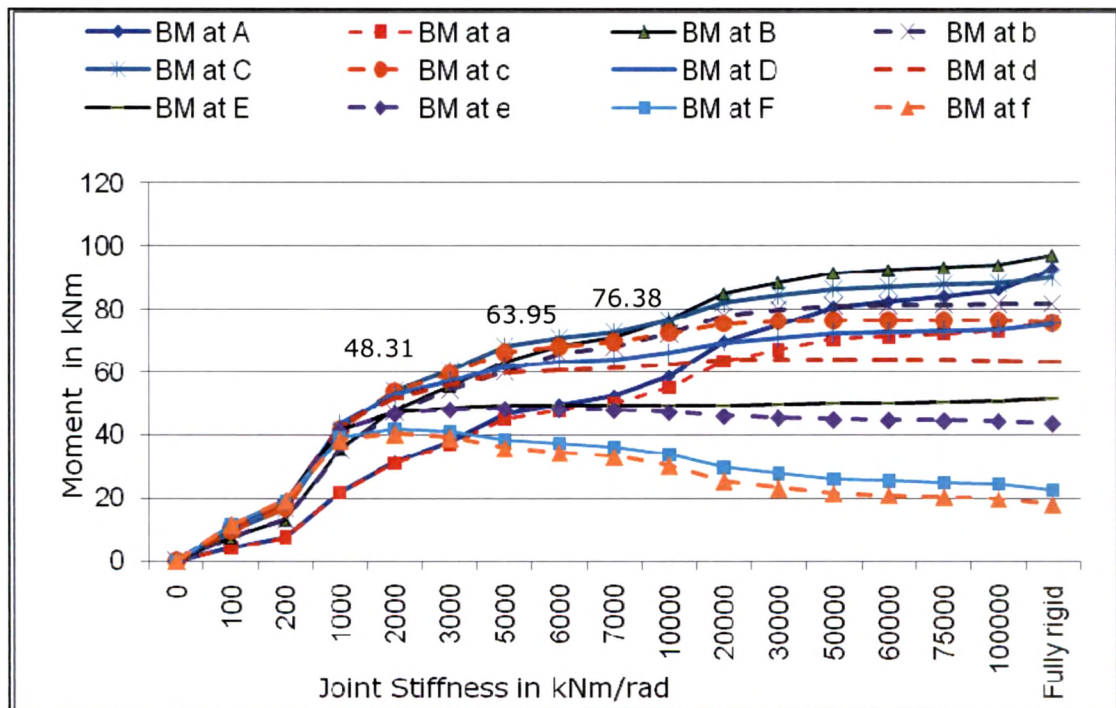


Fig. 8.14 Variation of EQ. Moment for a 6 Storey 2 bay Frame

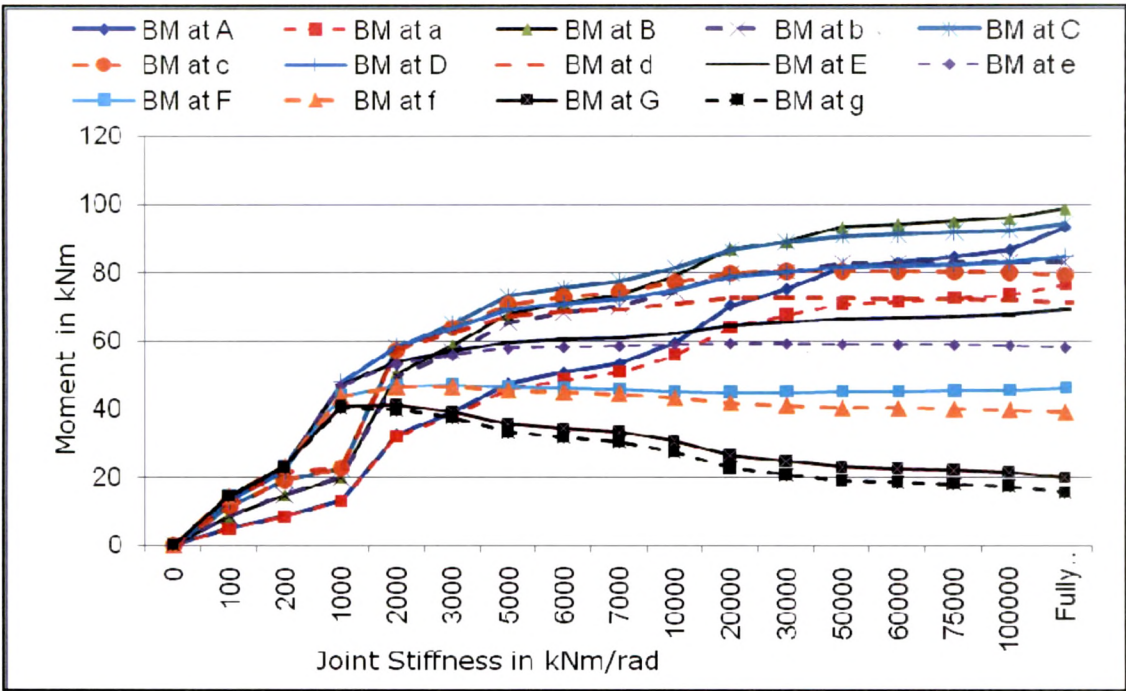


Fig. 8.15 Variation of EQ. Moment for a 7 Storey 2 Bay Frame

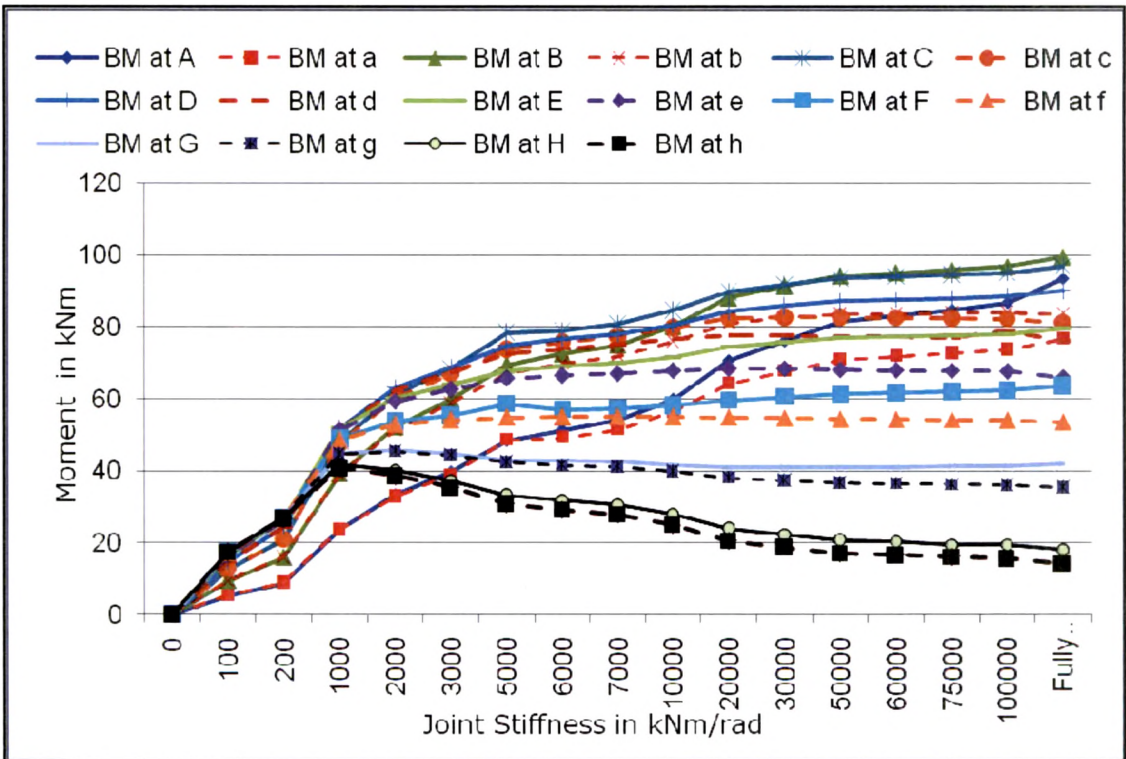


Fig. 8.16 Variation of EQ. Moment for a 8 Storey 2 Bay Frame

The results obtained for all the single bay frames are summarized in **Table 8.11**. The shaded values indicate the highest moments developed in frames with semi rigid joints. **Table 8.12** shows the ratio of the peak moments to that noted for the same frame considering all the joints as fully rigid. Thus, the ratios are indicated only corresponding to the shaded areas in **Table 8.11**. For the rest of the levels, the peak moment is observed because of fully rigid joints only. It may be noted that for 6, 7 and 8 storey frames, the top two storey show peak moment for frames with semi rigid joints exceeds that due to fully rigid joints.

Table 8.11 Value of Earthquake Moments for Single Bay Frames

Storey & Joint	Highest Earthquake Moment under Varying Rigidity							
	1	2	3	4	5	6	7	8
8th H								38.4
7th G							40.04	43.05
6th F						39.98	45.41	55.13
5th E					39.86	47.44	61.25	68.92
4th D				40.22	52.19	66.66	74.62	78.26
3rd C			40.32	59.19	72.59	79.23	82.77	83.91
2nd B		44.76	66.93	78.11	82.81	85.08	86.24	86.06
1st A	40.37	68.23	87.68	77.95	78.9	79.36	79.56	78.92

Table 8.12 Earthquake Moment Ratios for Single Bay Frames

Storey & Joint	Ratio of Peak Moment to fully Rigid Moment							
	1	2	3	4	5	6	7	8
8th H								2.46
7th G							2.17	1.18
6th F						1.92	1.08	NA
5th E					1.67	1.02	NA	NA
4th D				1.45	NA	NA	NA	NA
3rd C			1.21	NA	NA	NA	NA	NA
2nd B		1.12	NA	NA	NA	NA	NA	NA
1st A	NA	NA	NA	NA	NA	NA	NA	NA

Similarly for the two bay frames, the moments at points **A** thru **H** which are representing the outer joint shown in **Fig. 8.3** are presented in a compact form in **Table 8.13**. This table presents the value of the highest moment developed at the designated joint regardless of the rigidity at which they develop. The earthquake moment values which are shaded are those which are developed in semi rigid frames and the other values are those which are developed in fully rigid frames. The earthquake moments developed at the points marked by shaded area due to full rigidity of the frames are also noted and the ratio of the peak moments due to semi rigid joints to those developed due to fully rigid joints is presented in **Table 8.14**. Thus, in **Table 8.14**, the cells indicating NA are the ones where the peak moments develop due to fully rigid joints only. Similar concept is adopted at the inner joint marked as points **a** thru **h** as indicated in **Fig. 8.3** for the two bay frames. The peak earthquake moments are presented in **Table 8.15** and the moment ratio of the peak moment to fully rigid moment is noted in **Table 8.16**. It may be noted here that the peak moment at the external joint and the internal joint may not occur at the same level of semi rigidity. The values are noted down and plotted for all the frames which reveals a lot of useful information about the behavior of RC plane frames having semi rigid joints.

Table 8.13 Earthquake Moments at Outer Joint for Two Bay Frames

Storey & Joint	Highest Earthquake Moment under Varying Rigidity							
	1	2	3	4	5	6	7	8
8th H								41.7
7th G							41.28	45.88
6th F						41.86	47.23	63.74
5th E					42.03	51.66	69.15	79.54
4th D				42.41	58.14	75.32	84.69	90.21
3rd C			43.27	86.12	82.14	89.99	94.22	96.71
2nd B		45.54	75.15	88.62	94.28	97.03	98.52	99.42
1st A	3.52	78.62	87.68	90.77	92.09	92.77	93.14	93.4

Table 8.14 Earthquake Moment Ratios for Two Bay Frames

Storey & Joint	Ratio of Peak Moment to fully Rigid Moment							
	1	2	3	4	5	6	7	8
8th H								2.31
7th G							2.05	1.09
6th F						1.84	1.01	NA
5th E					1.61	NA	NA	NA
4th D				1.38	NA	NA	NA	NA
3rd C			1.17	NA	NA	NA	NA	NA
2nd B		1.02	NA	NA	NA	NA	NA	NA
1st A	NA	NA	NA	NA	NA	NA	NA	NA

Table 8.15 Earthquake Moments at Inner Joint of Two Bay Frames

Storey & Joint	Highest Earthquake Moment under Varying Rigidity							
	1	2	3	4	5	6	7	8
8th h								40.88
7th g							40.17	45.43
6th f						40.36	46.57	55.05
5th e					39.93	48.31	59.16	68.45
4th d				39.34	51.23	63.95	72.51	78.85
3rd c			38.81	55.68	69.17	76.36	80.38	82.85
2nd b		37.71	63.19	74.39	79.38	81.76	83.05	83.82
1st a	1.43	63.76	71.46	74.33	75.51	76.11	76.44	76.66

Table 8.16 Earthquake Moment Ratios for Two Bay Frames

Storey & Joint	Ratio of Peak Moment to fully Rigid Moment							
	1	2	3	4	5	6	7	8
8th h								2.89
7th g							2.55	1.27
6th f						2.27	1.18	1.02
5th e					1.96	1.1	1.01	1.03
4th d				1.65	1.04	1.01	1.01	1.03
3rd c			1.36	NA	1.01	1	1.01	1.01
2nd b		1.09	NA	NA	NA	NA	NA	NA
1st a	-1.72	NA	NA	NA	NA	NA	NA	NA

8.4 EFFECT OF SEMIRIGID JOINTS ON SEISMIC PERFORMANCE

It is clear from the study presented in the previous section that as the rigidity of the joints increases from zero (pinned condition) to very high (fully rigid condition), the earthquake moments developed at the terrace level beams show a peak value of moment. This leads to the fact that the stress developed in a plastic hinge defined at these points will be higher than those which would have developed if the frame had been considered as fully rigid.

Thus, for all the models, the rigidity at which a peak moment is observed is noted down. It is interesting to see that for a particular frame, there can be one value of rigidity at which the outer joint may exhibit a peak value of moment and another value of rigidity at which the inner joint may show a peak value. Thus, all the rigidities at which a peak moment is developed anywhere in the model is noted down for that particular model. Next, the model is subjected to pushover analysis with all the joints having the rigidity corresponding to the ones noted down for peak values. The default PMM (combined axial and flexural) hinges are defined in SAP2000 software model at the ends of all beams and columns. There are two pushover cases defined for each analysis. The first push is given in the gravity direction defined as PUSH1 up to the full magnitude of the gravity loads. Next, the stresses developed in each of the hinges are superimposed by the stress due to lateral push defined as PUSH2. The lateral push is displacement controlled up to a total displacement of an identified roof level node to undergo a total lateral displacement of 0.04 times the height of the frame. The performance point obtained by superimposing the capacity spectra on to the demand spectra for each frame in the ADRS format is noted down for each case. The results of the

pushover analysis are presented as a deformed shape of all the frames under lateral push with colour coded hinges shown for each frame.

The results consist of a deformed shape for 1 storey plane frames with 1 storey to 8 storey with colour coded hinges along with the first hinge marked as 1. These are presented as **Figs. 8.17, 8.18, 8.20, 8.22, 8.24, 8.26, 8.28 and 8.30**. These figures contain the deformed shape for different rigidities considered along with a fully rigid case.

The graph showing the performance point obtained as an intersection of the capacity spectrum with the demand spectrum for each case of rigidity including the fully rigid case is presented for single bay frames in **Figs. 8.17, 8.19, 8.21, 8.23, 8.25, 8.27, 8.29 and 8.31**. These graphs also indicate family of demand spectra for 5, 10, 15 and 20% damping, the demand being determined by IS 1893 Part1, 2002 [24] spectrum. The graph of spectral acceleration versus spectral displacement in ADRS format shown in the above figures also show radial lines corresponding to constant periods.

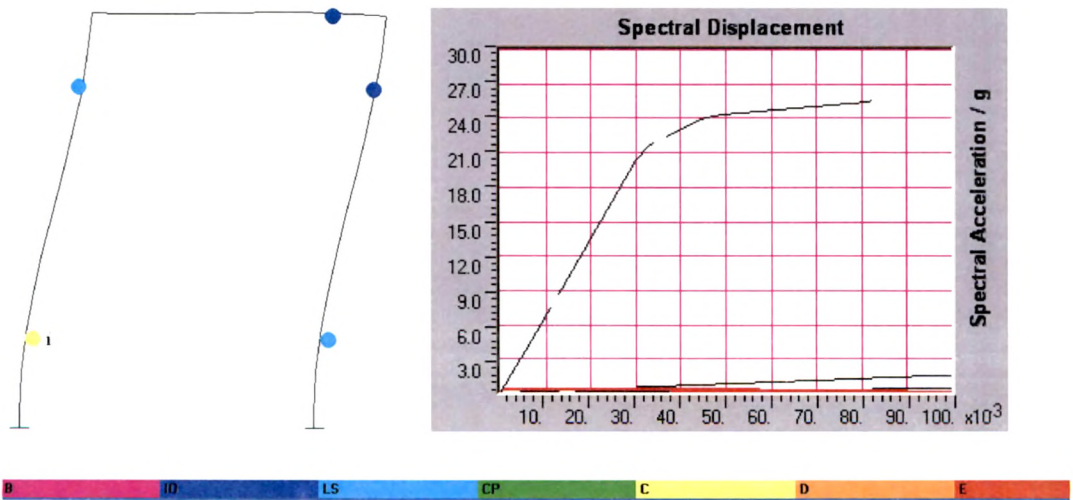


Fig. 8.17 Push Over Curve and Deformation for Fully Rigid Frame

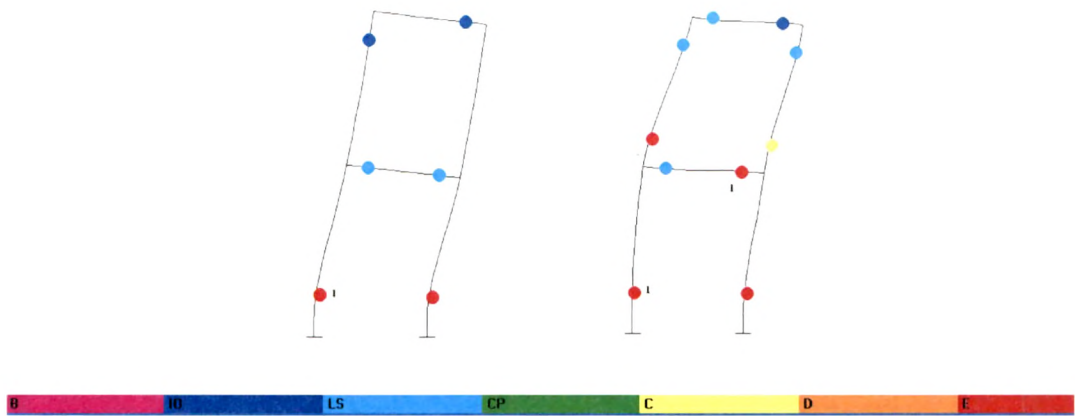


Fig. 8.18 Push at 50000 kNm/rad and Full Rigidity Deformed Shape

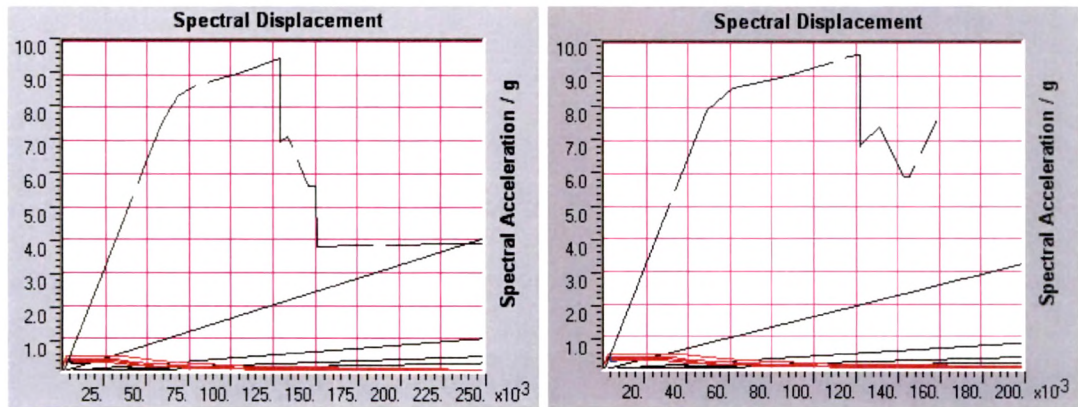


Fig. 8.19 Performance Point at 50000 kNm/rad and Full Rigidity

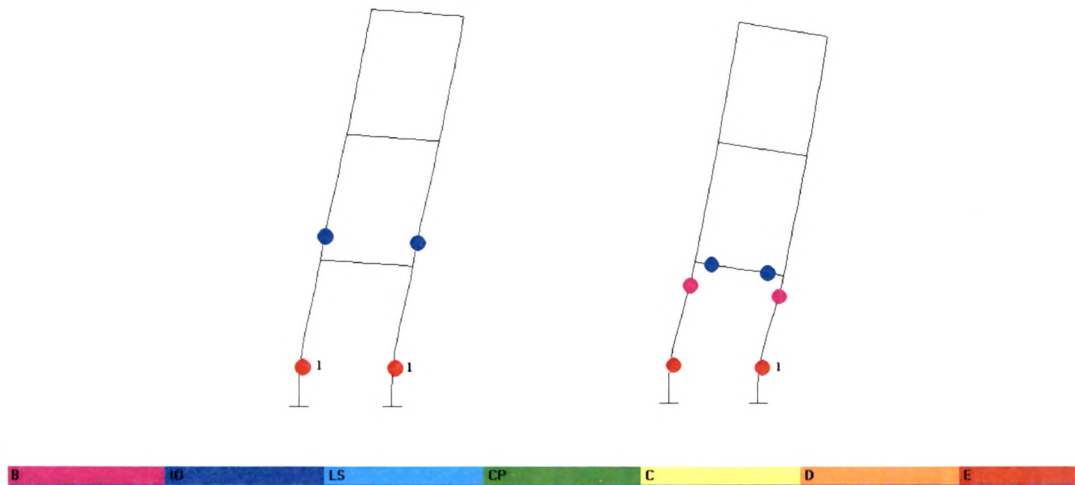


Fig. 8.20 Push at 10000 kNm/rad and Full Rigidity

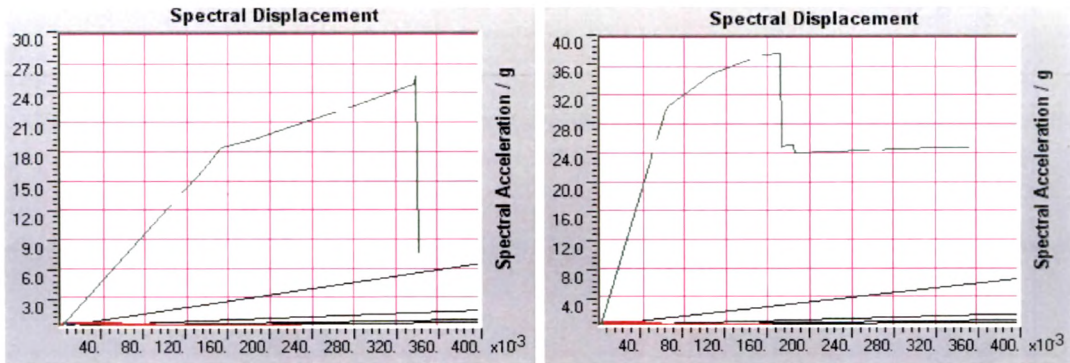


Fig. 8.21 Performance Point at 10000 kNm/rad and Full Rigidity

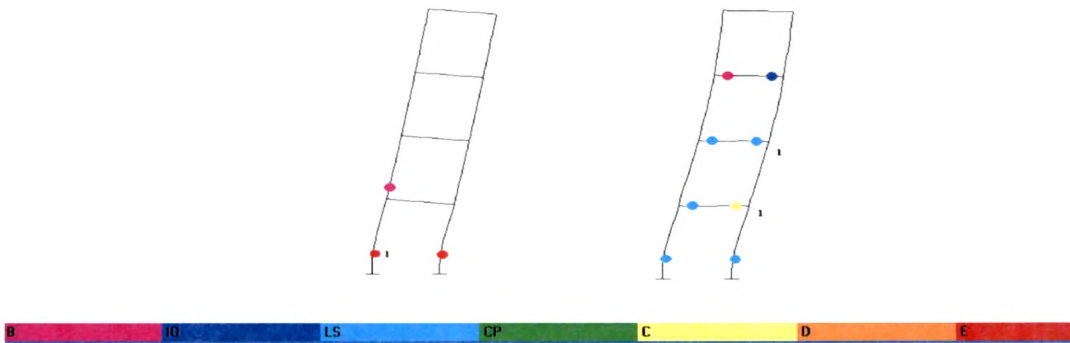


Fig. 8.22 Push at 6000 kNm/rad and Full Rigidity

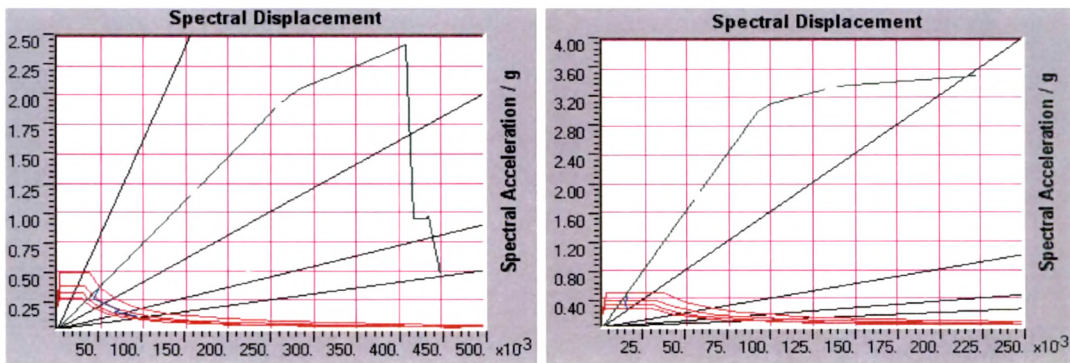


Fig. 8.23 Performance Point at 6000 kNm/rad and Full Rigidity

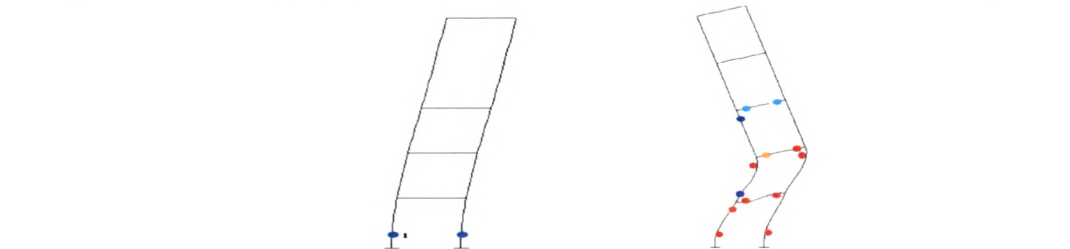


Fig. 8.24 Push at 3000 kNm/rad and Full Rigidity

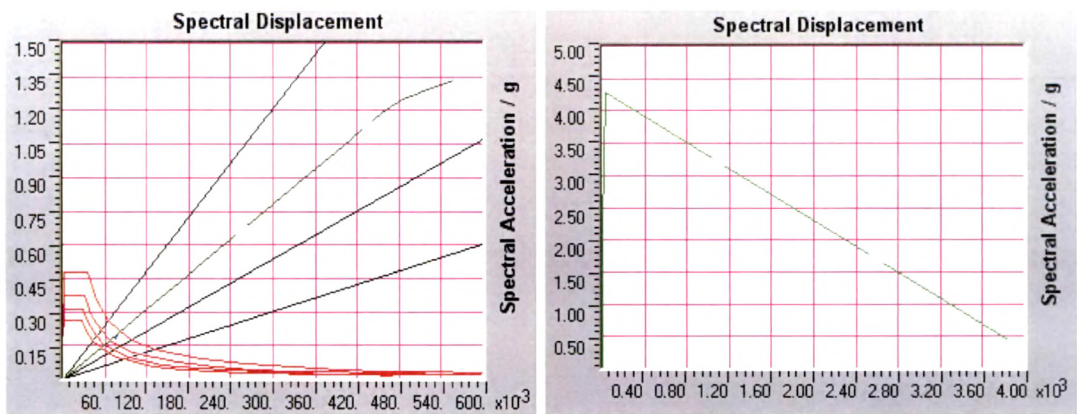


Fig. 8.25 Performance Point at 3000 kNm/rad and Full Rigidity

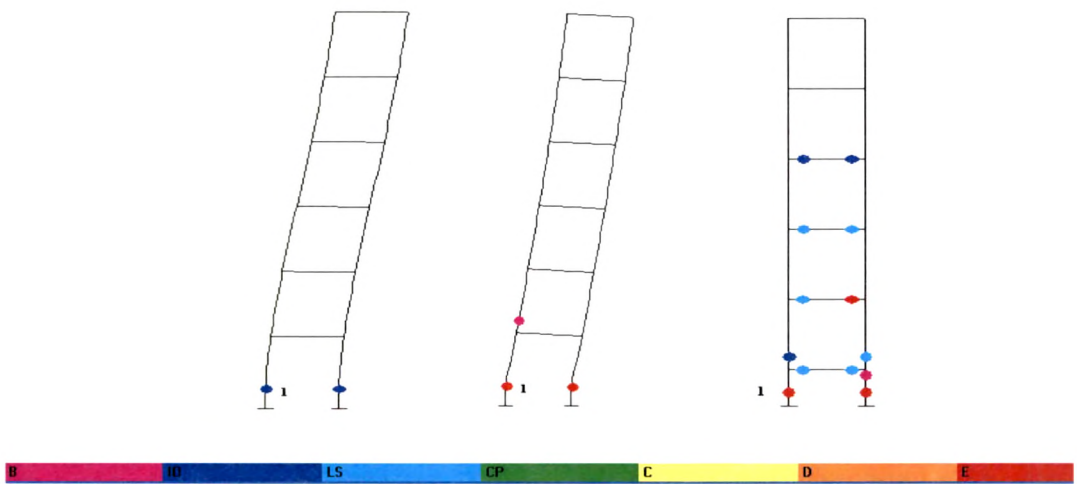


Fig. 8.26 Push at 3000, 7000 kNm/rad and Full Rigidity

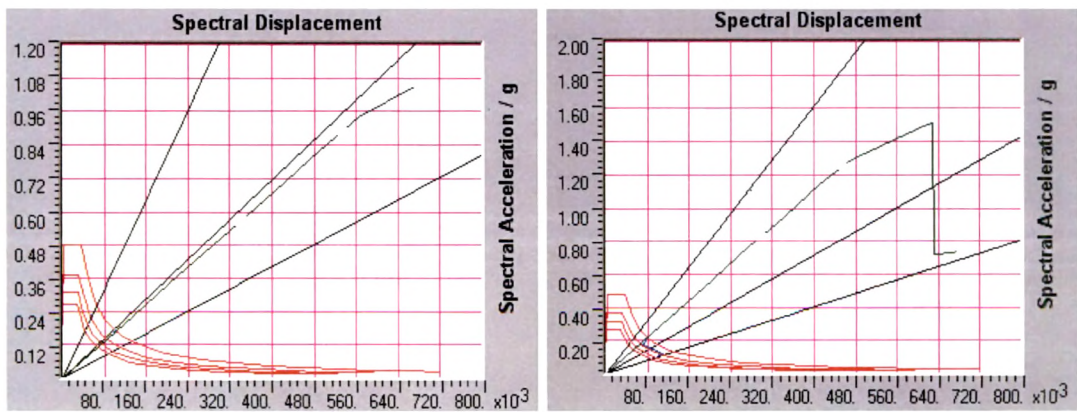


Fig. 8.27a Performance Point at 3000 and 7000 kNm/rad Rigidity

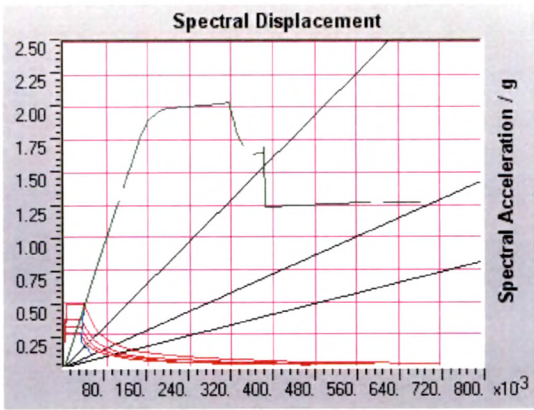


Fig. 8.27b Performance Point at Full Rigidity

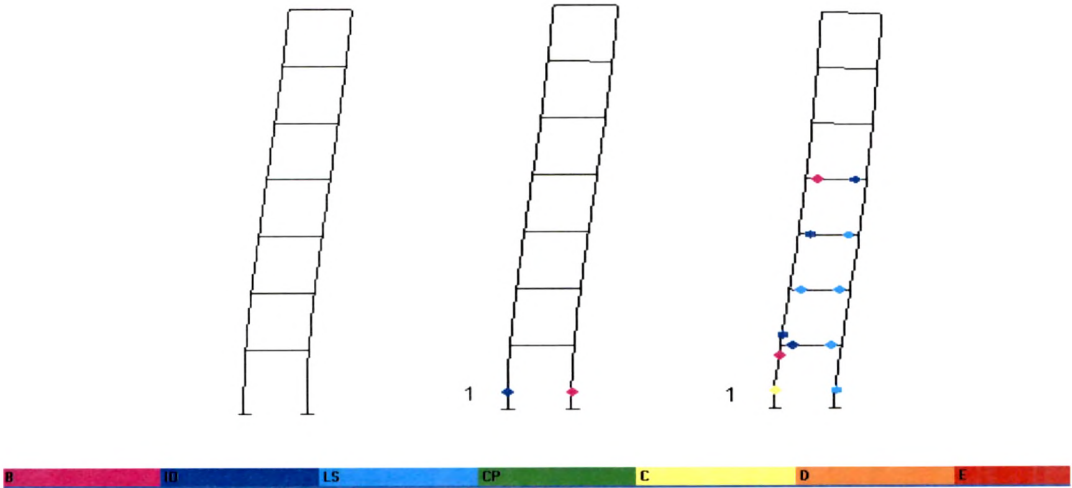


Fig. 8.28 Push at 2000, 3000 kNm/rad and Full Rigidity

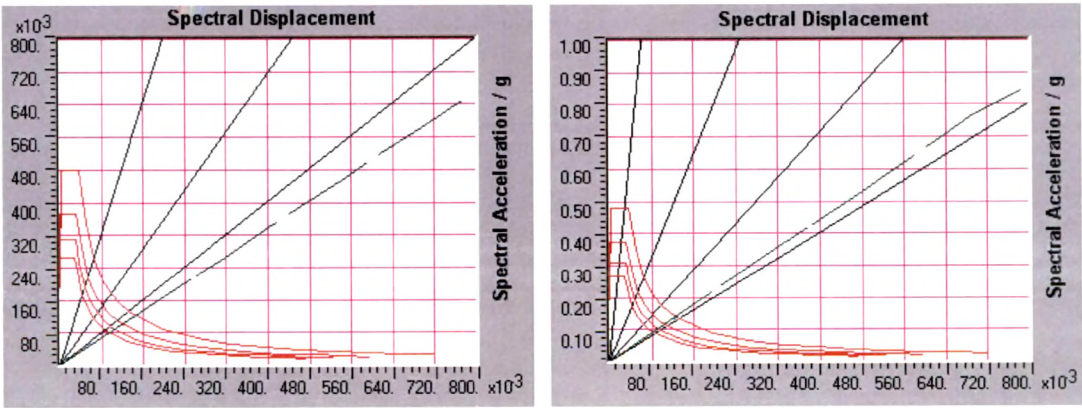


Fig. 8.29a Performance Point at 2000 and 3000 kNm/rad Rigidity

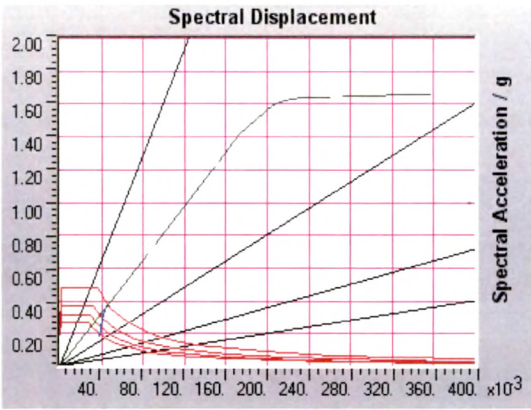


Fig. 8.29b Performance Point at Full Rigidity

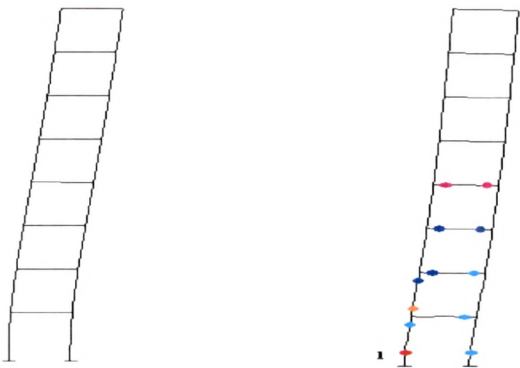


Fig. 8.30 Push at 2000 kNm/rad and Full Rigidity

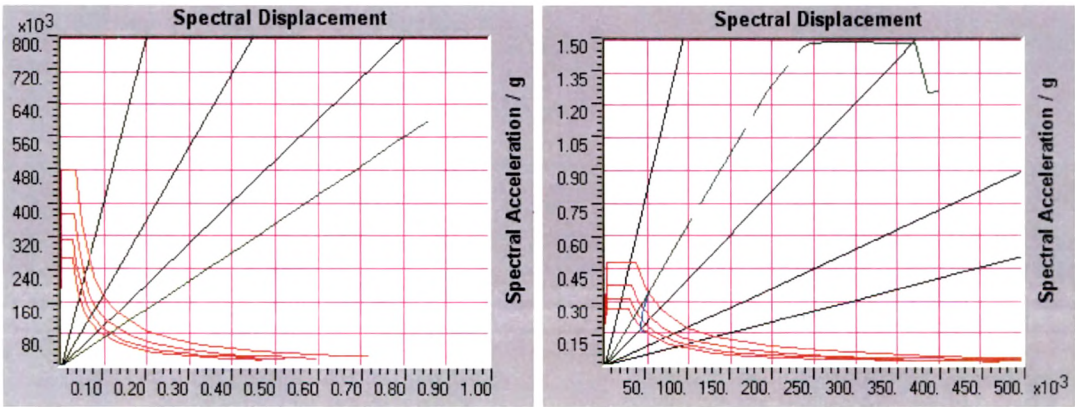


Fig. 8.31 Performance Point at 2000 kNm/rad and Full Rigidity

The important parameters observed at performance point for single bay frames of 1 storey to 8 storey are summarized in **Table 8.17**. The parameters noted down in the table are base shear V , roof displacement D , spectral acceleration S_a , spectral displacement S_d , effective time period T_{eff} and effective damping β_{eff} at performance point. The values of base shear and roof displacement at performance point for various rigidities of beam joints used for each model are plotted in **Fig. 8.32**.

Table 8.17 Values at Performance Point for Single Bay Frames

Storey	Rigidity (kN-m/rad)	V (kN)	D (m)	S _a (g)	S _d (m)	T _{eff} (sec)	β _{eff} (%)
2	Full	17.5	0.004	0.480	0.003	0.158	5.0
	50000	17.1	0.005	0.480	0.004	0.177	5.0
3	Full	13.9	0.001	0.432	0.001	0.091	5.0
	10000	14.1	0.006	0.480	0.004	0.184	5.0
4	Full	37.4	0.020	0.480	0.015	0.353	5.0
	6000	25.8	0.068	0.357	0.048	0.739	5.0
5	Full	44.9	0.064	0.863	0.046	0.464	5.0
	3000	19.0	0.117	0.213	0.081	1.241	5.0
6	Full	53.5	0.053	0.495	0.038	0.580	5.0
	7000	24.5	0.111	0.219	0.079	1.210	5.0
	3000	18.4	0.146	0.170	0.102	1.550	5.0
7	Full	51.1	0.065	0.375	0.046	0.704	5.0
	3000	17.7	0.178	0.138	0.125	1.907	5.0
	2000	15.2	0.208	0.120	0.144	2.192	5.0
8	Full	48.4	0.077	0.337	0.051	0.783	5.0
	2000	14.7	0.238	0.110	0.156	2.395	5.0

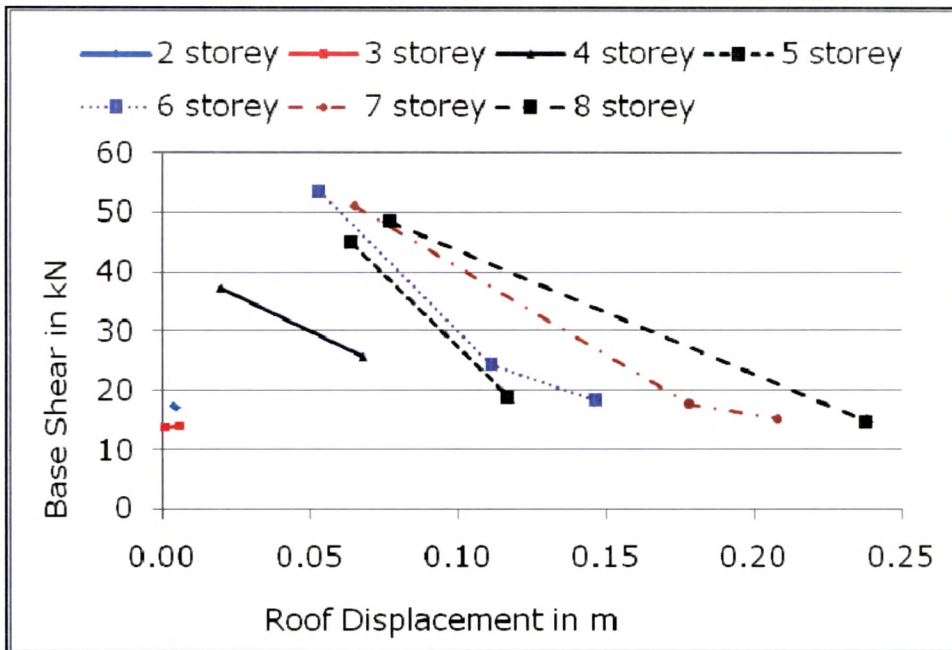


Fig. 8.32 Performance Point Variation with Rigidity – Single Bay

The 2 bay frames ranging from 1 storey to 8 storey are analyzed under push over procedure and the various parameters are noted down at performance point. Mathematical models are developed for each of the frames with beam end rigidities corresponding to the peak moment exhibited in the previous analysis. The results obtained for various semi rigid joint cases are compared to the same frame having all the joints as fully rigid as considered in a conventional frame analysis. The push over cases are defined in the usual manner with the first push being applied in the gravity direction and then the lateral push is started. The local redistribution is applied to the structure when a hinge drops load. The other parameters considered for push over analysis are building type B and medium soil conditions. The earthquake loads are considered as per IS 1893, part1, 2002. The deformed shape along with colour coded hinges developed in each of the frame models are presented in **Figs. 8.33, 8.35,**

8.37, 8.39, 8.41, 8.43, 8.45 and **8.47**. The first hinge developed in each of the model is indicated by 1 besides the hinge.

The graph of spectral acceleration versus spectral displacement in ADRS format for each of the mathematical model is recorded and presented as **Figs. 8.34, 8.36, 8.38, 8.40, 8.42, 8.44, 8.46** and **8.48**. Apart from the performance point represented by the intersection of capacity spectrum with single demand spectrum with variable damping, the graphs also contain the family of demand spectra for 5, 10, 15 and 20 % damping shown in red. The radial lines emanating from the origin are the constant period lines. Thus, important information is contained in the graphs which indicate the general behavior of the model under seismic loads. The results in the form of base shear V, roof level displacement D, spectral acceleration and displacements Sa and Sd, the effective time period T_{eff} and the effective damping β_{eff}, at performance point are summarized in **Table 8.18**. A graph of roof displacement versus base shear for all the models is presented as **Fig. 8.49**.

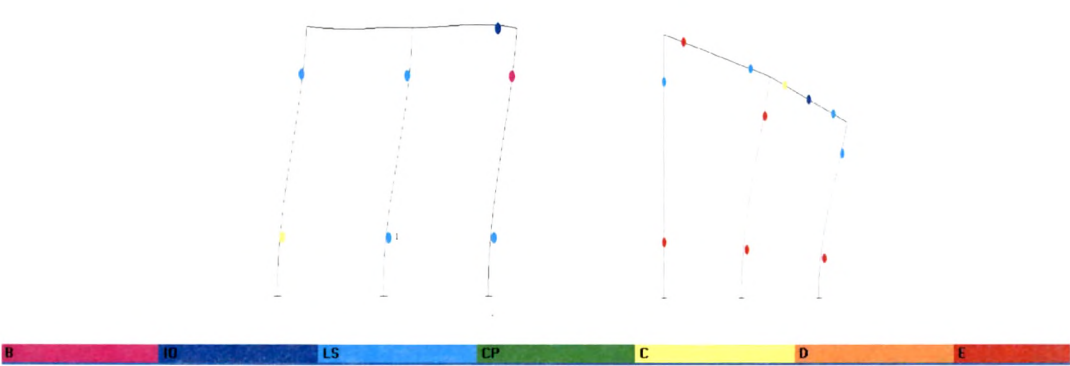


Fig. 8.33 Push at 10000 kNm/rad and Full Rigidity

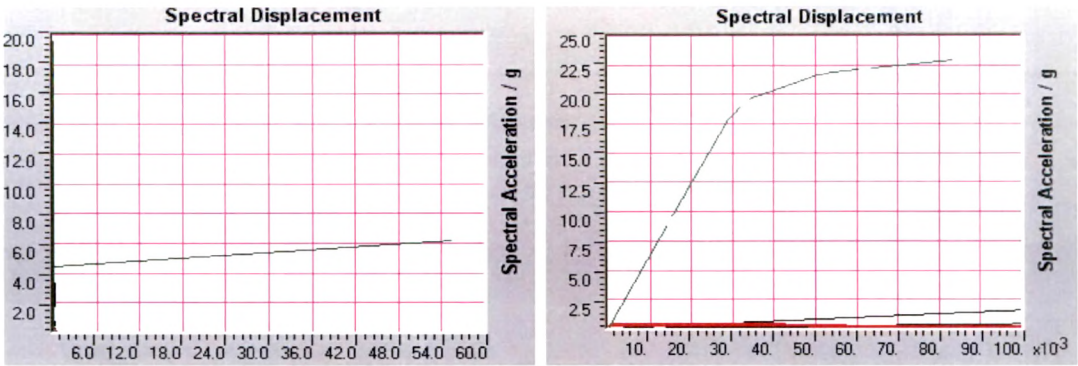


Fig. 8.34 Performance Point at 10000 kNm/rad and Full Rigidity

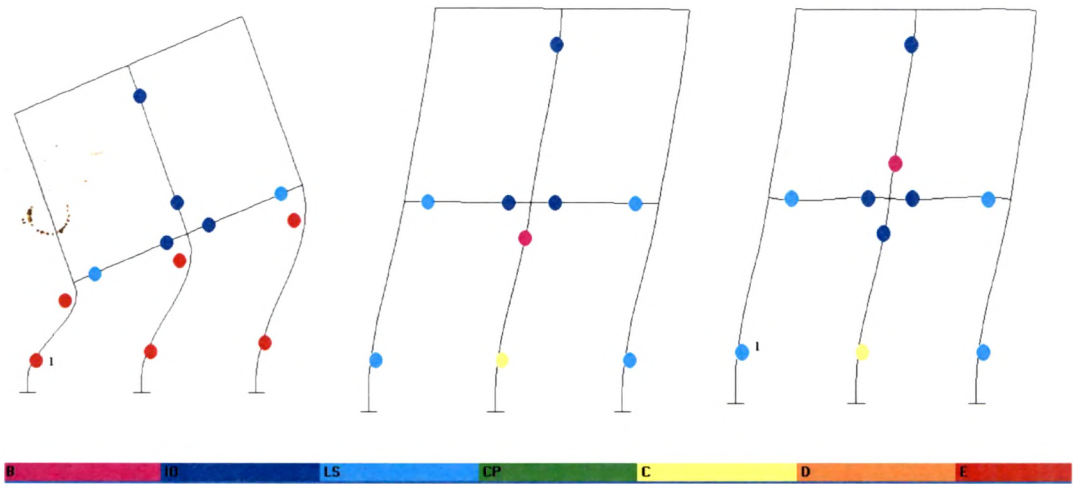


Fig. 8.35 Push at 20000, 50000 kNm/rad and Full Rigidity

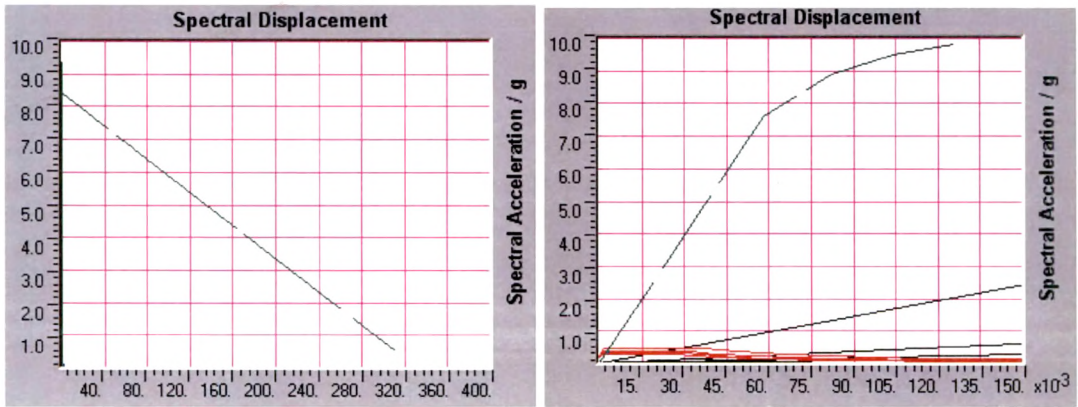


Fig. 8.36 Performance Point at 20000 and 50000 kNm/rad Rigidity

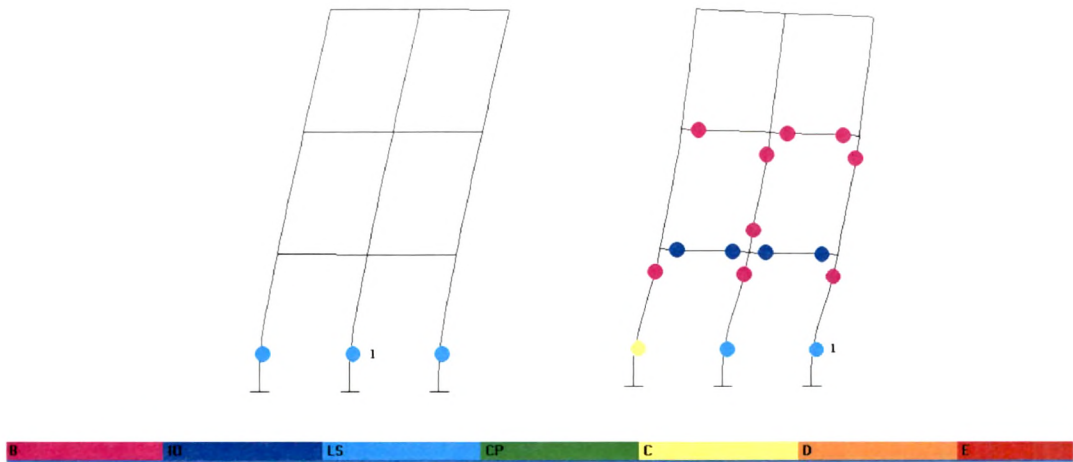


Fig. 8.37 Push at 7000 kNm/rad and Full Rigidity

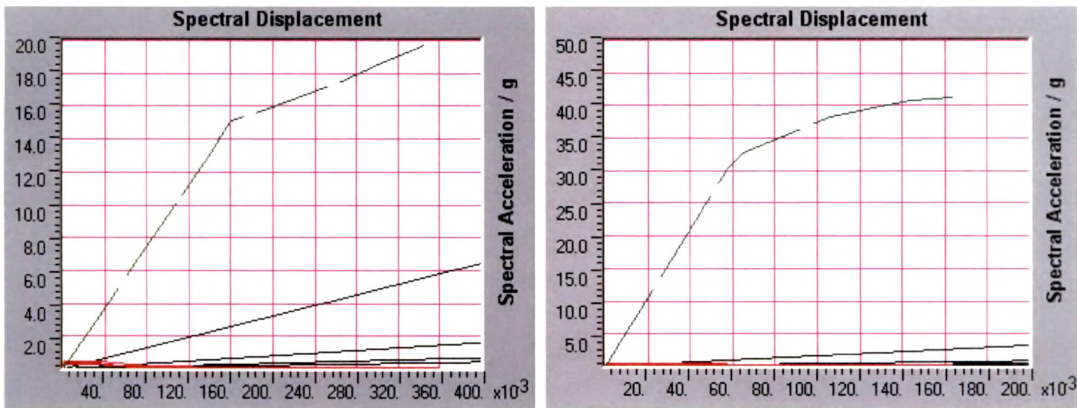


Fig. 8.38 Performance Point at 7000 kNm/rad and Full Rigidity

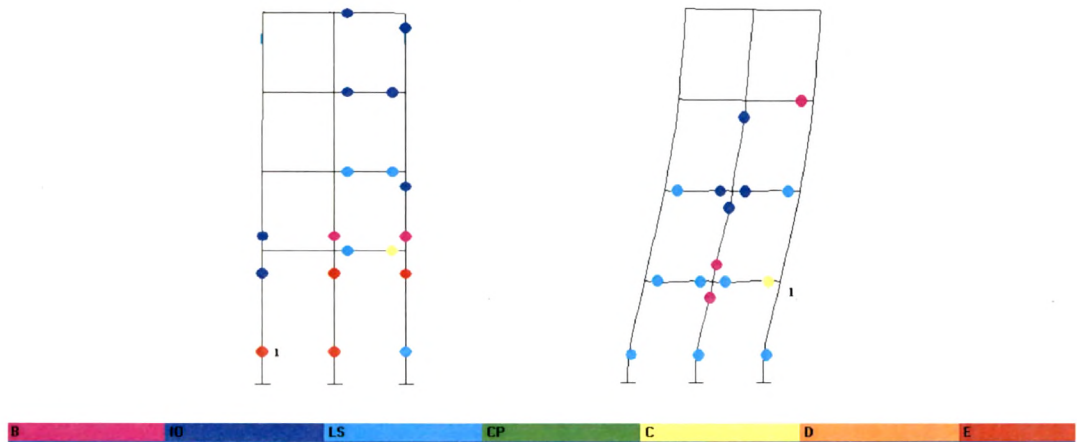


Fig. 8.39 Push at 5000 kNm/rad and Full Rigidity

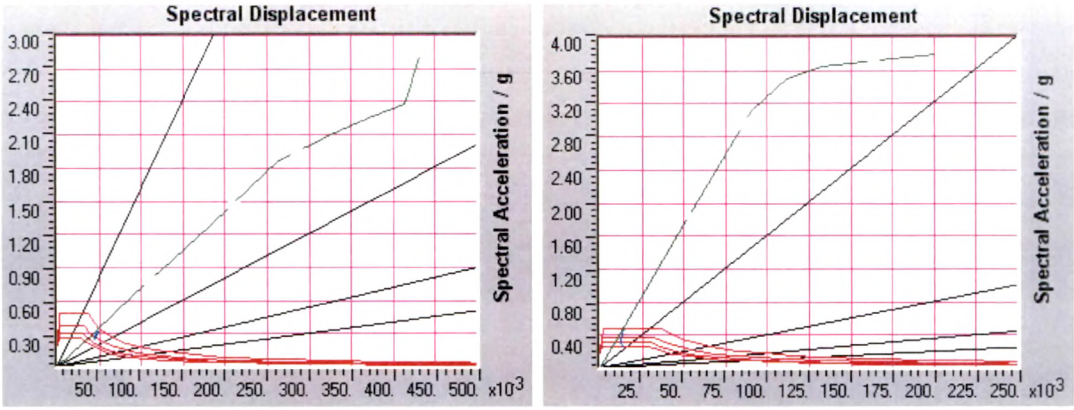


Fig. 8.40 Performance Point at 5000 kNm/rad and Full Rigidity

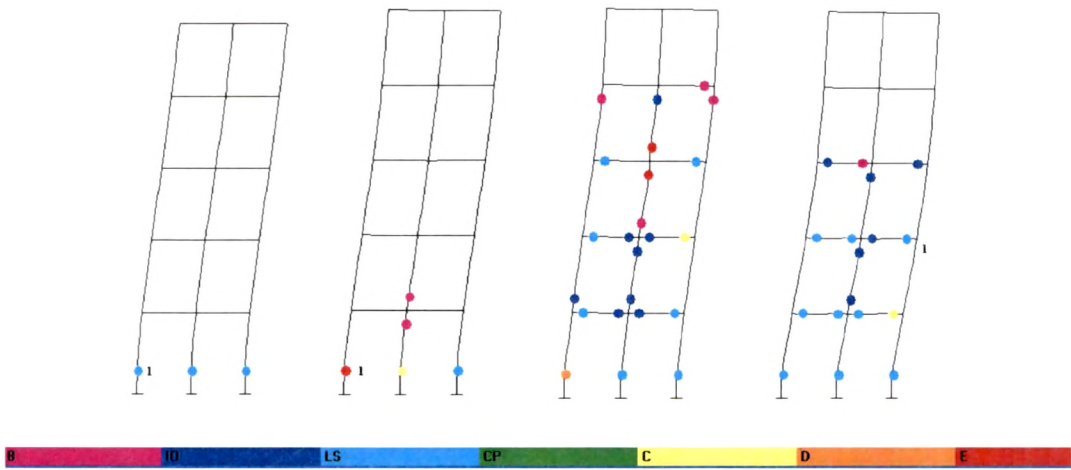


Fig. 8.41 Push at 3000, 10000, 75000 kNm/rad and Full Rigidity

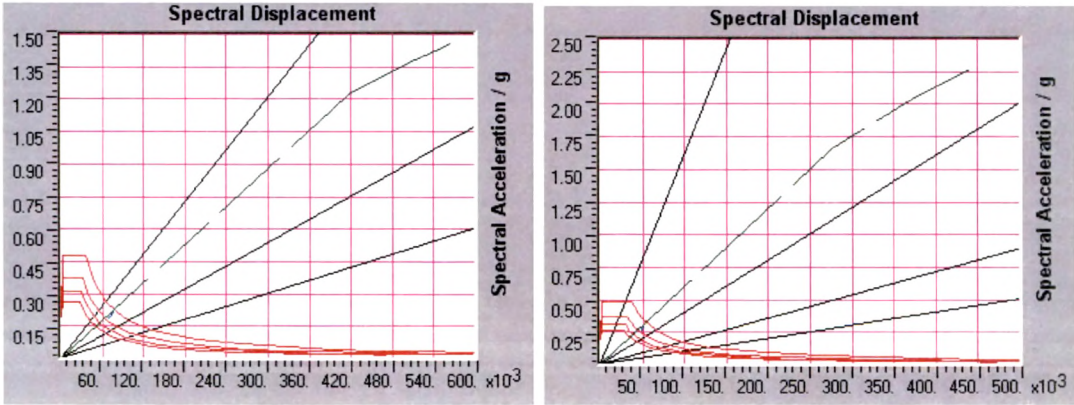


Fig. 8.42a Performance Point at 3000 and 10000 kNm/rad Rigidity

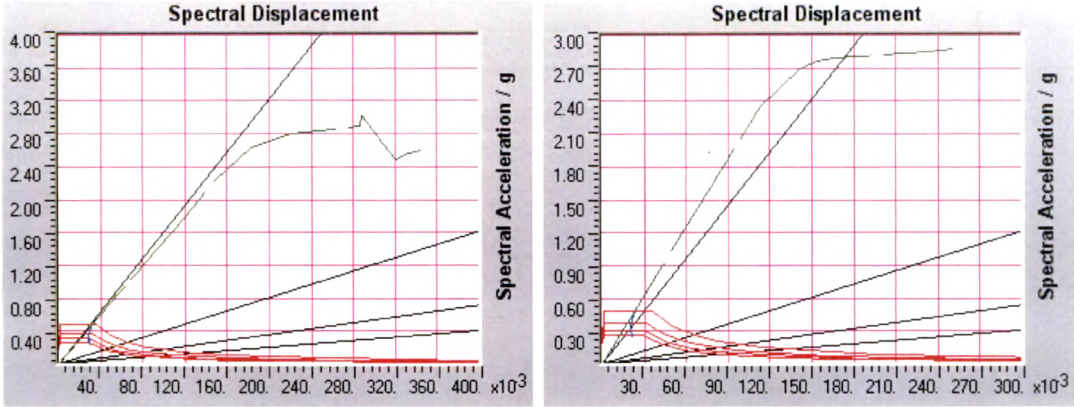


Fig. 8.42b Performance Point at 75000 kNm/rad and Full Rigidity

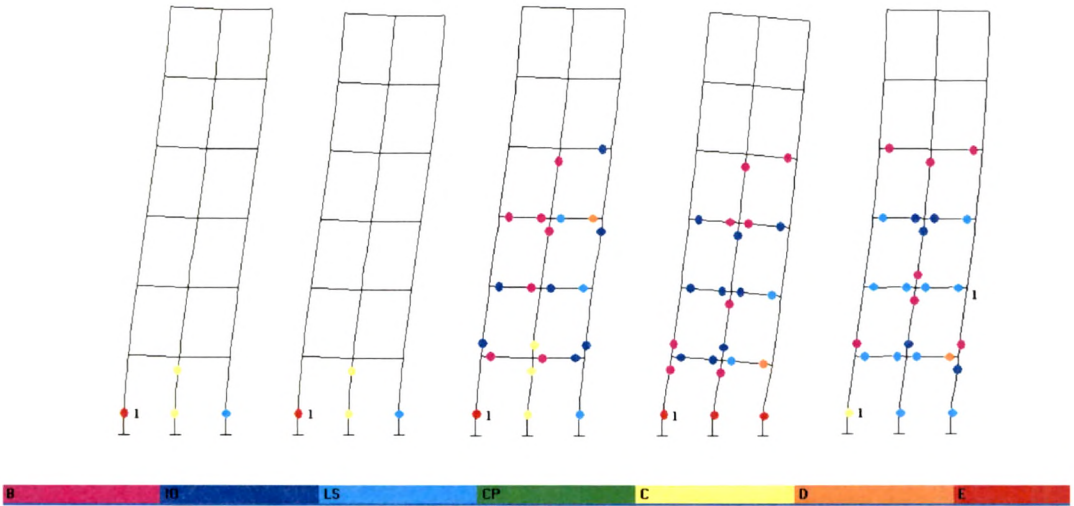


Fig. 8.43 Push at 2000, 5000, 30000, 50000 and Full Rigidity

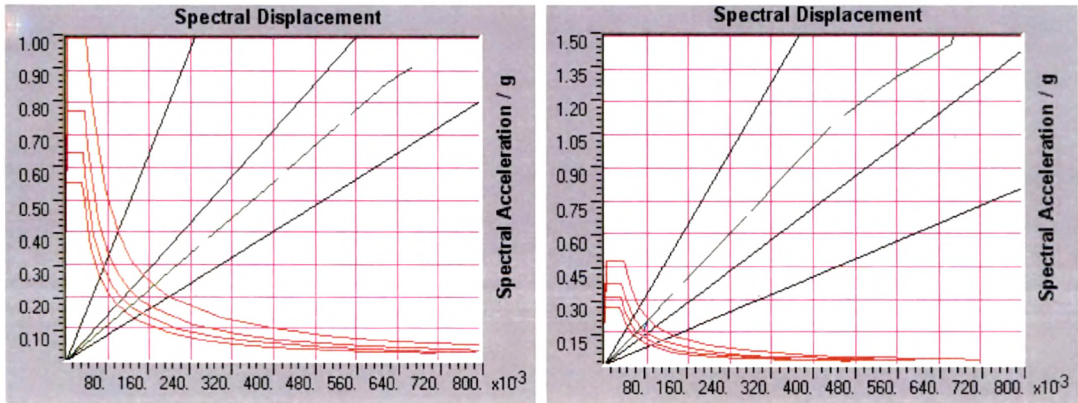


Fig. 8.44a Performance Point at 2000 and 5000 kNm/rad Rigidity

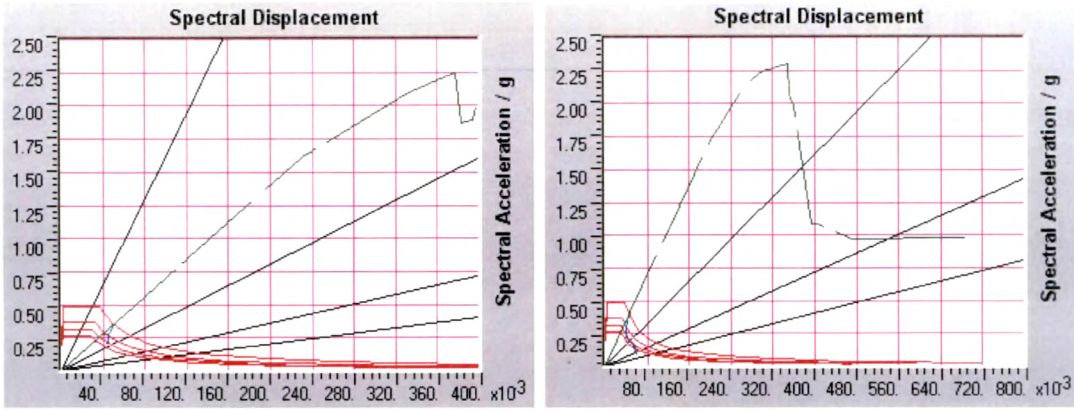


Fig. 8.44b Performance Point at 30000 and 50000 kNm/rad Rigidity

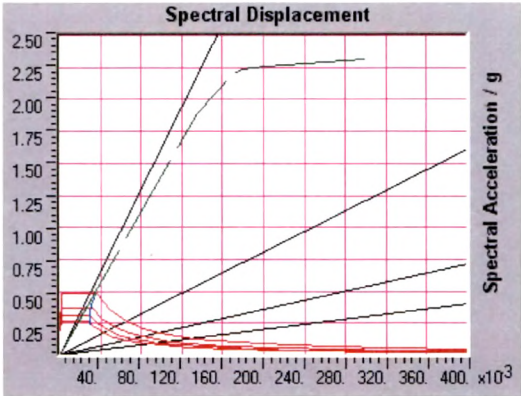


Fig. 8.44c Performance Point at Full Rigidity

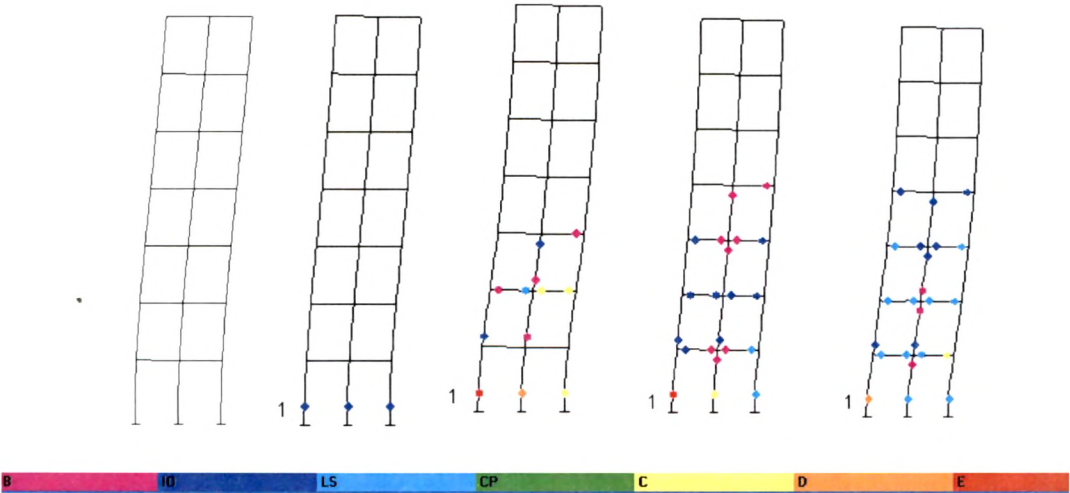


Fig. 8.45 Push at 1000, 2000, 3000, 20000 and Full Rigidity

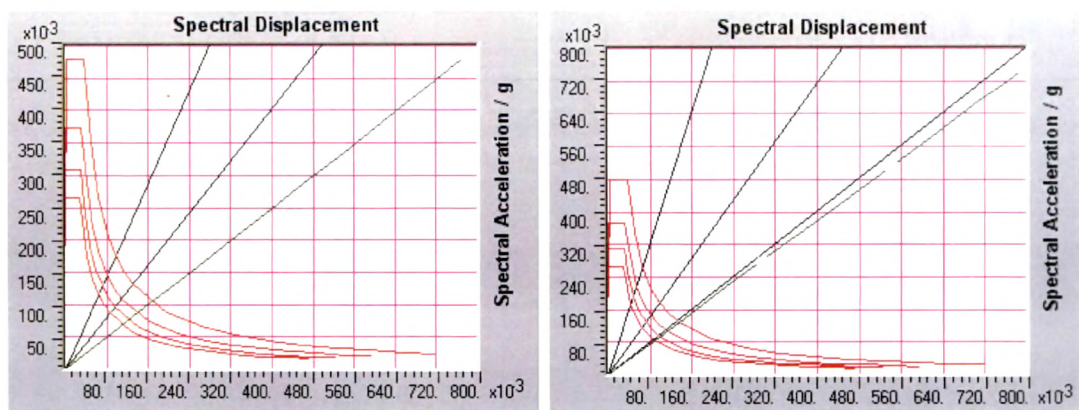


Fig. 8.46a Performance Point at 1000 and 2000 kNm/rad Rigidity

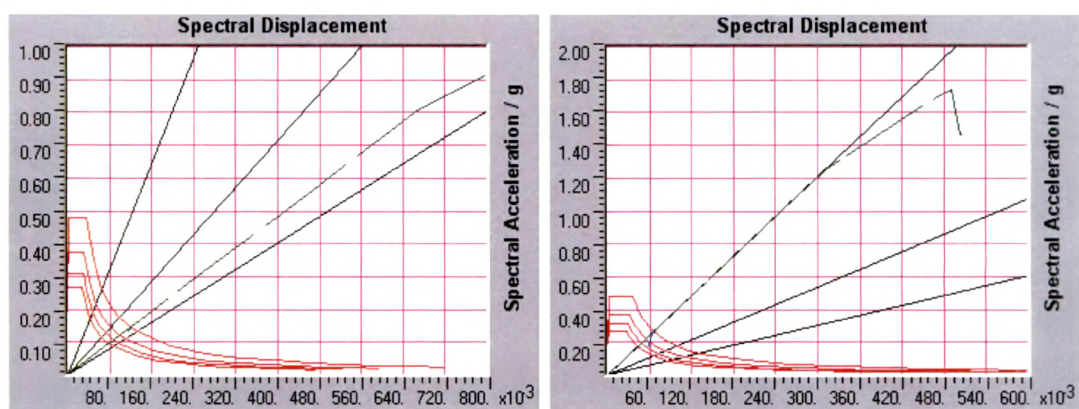


Fig. 8.46b Performance Point at 3000 and 20000 kNm/rad Rigidity

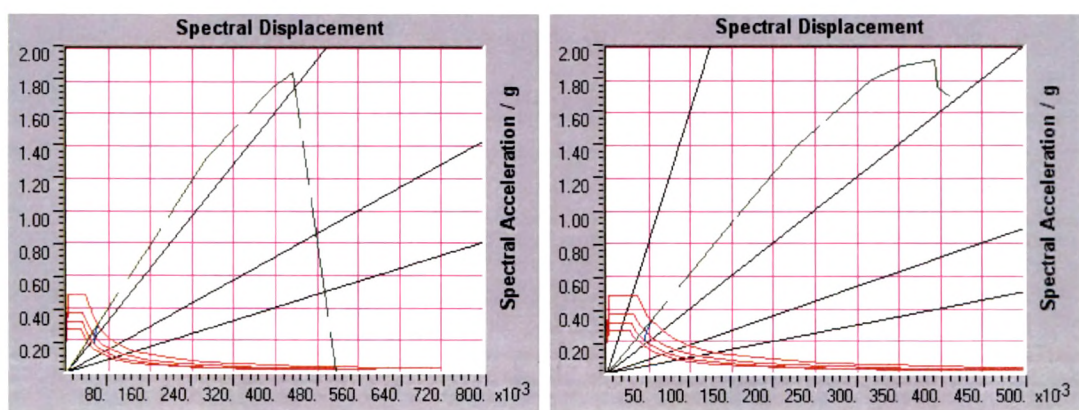


Fig. 8.46c Performance Point at 30000 and 50000 kNm/rad Rigidity

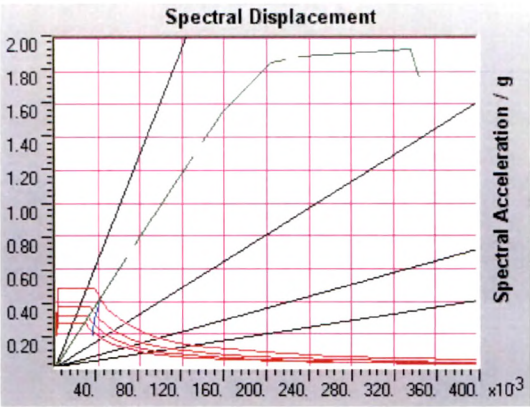


Fig. 8.46d Performance Point at Full Rigidity

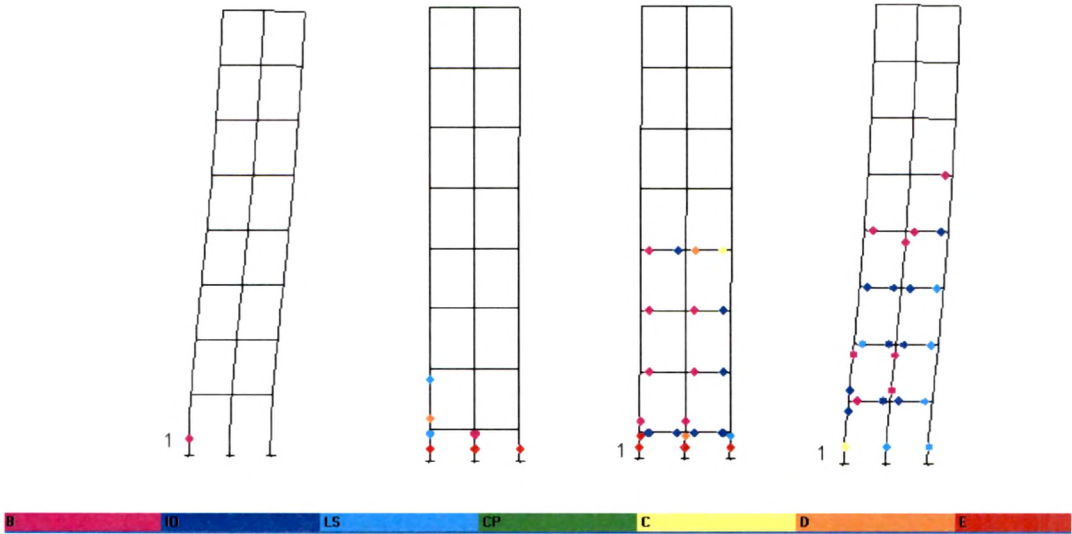


Fig. 8.47 Push at 10000, 20000, 30000 and Full Rigidity

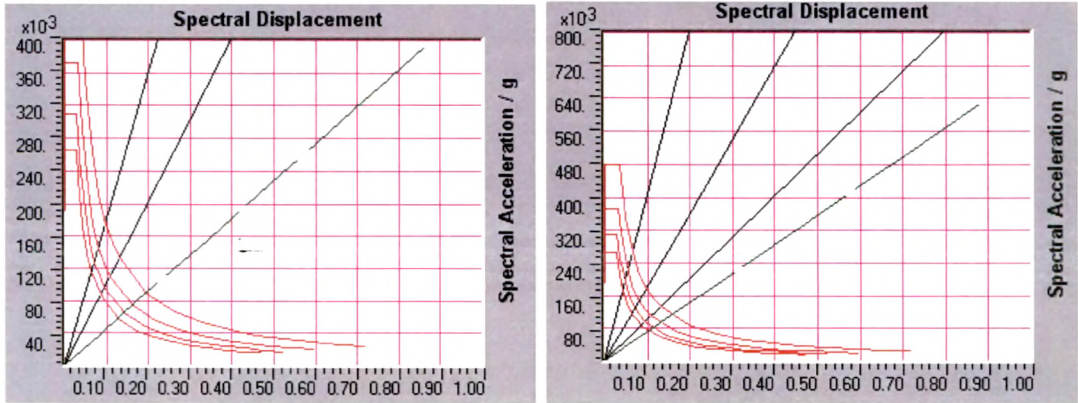


Fig. 8.48a Performance Point at 1000 and 3000 kNm/rad Rigidity

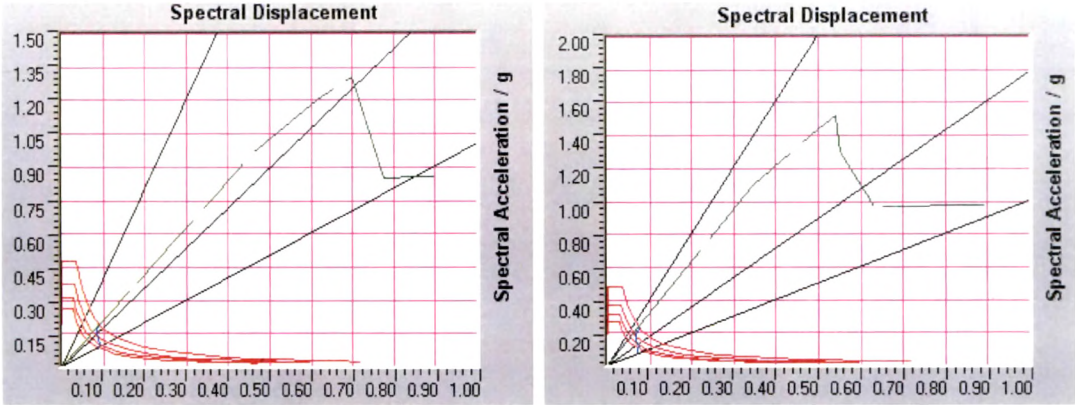


Fig. 8.48b Performance Point at 10000 and 20000 kNm/rad Rigidity

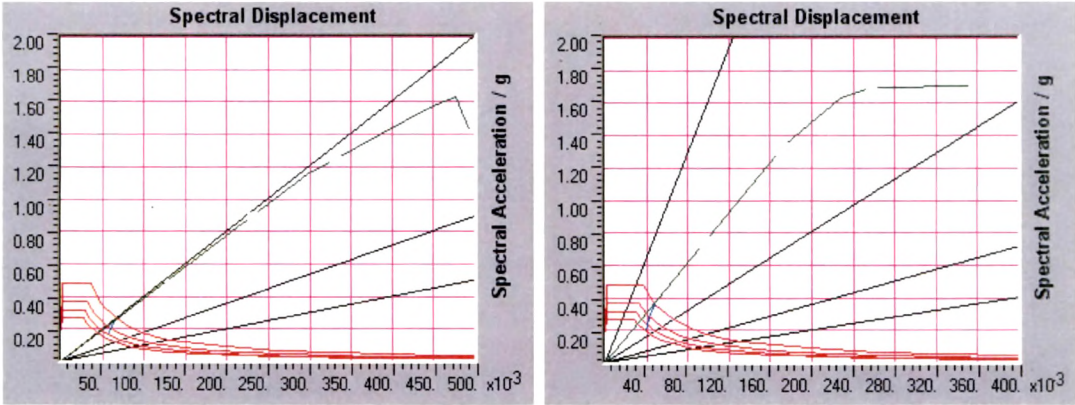


Fig. 8.48c Performance Point at 30000 kNm/rad and Full Rigidity

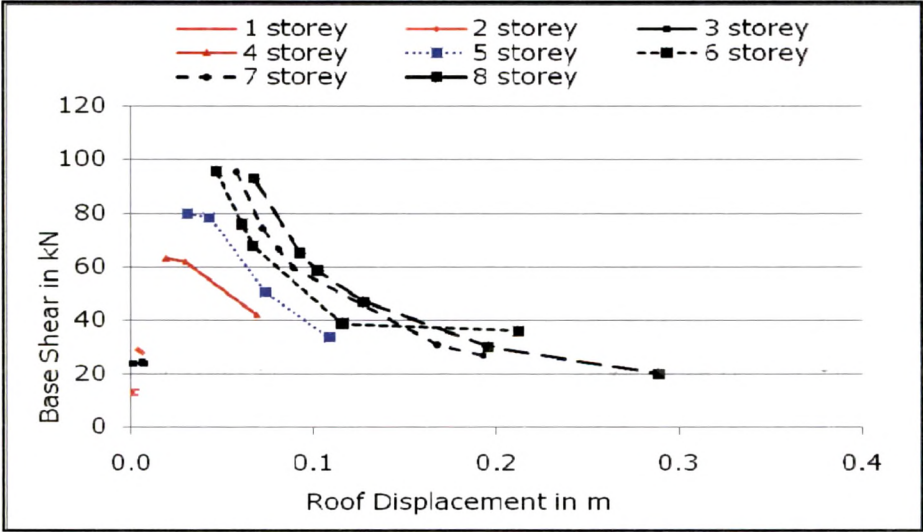


Fig. 8.49 Performance Point Variation with Rigidity – Two Bay Frames

Table 8.18 Values at Performance Point for Two Bay Frames

Storey	Rigidity (kN- m/rad)	V (kN)	D (m)	Sa (g)	Sd (m)	Teff (sec)	βeff (%)
1	Full	11.8	0.001	0.404	0	0.081	5
	10000	13.8	0.001	0.466	0.001	0.783	5
2	Full	29.1	0.004	0.48	0.003	0.158	5
	50000	28.6	0.005	0.48	0.004	0.176	5
	20000	27.9	0.006	0.48	0.005	0.204	5
3	Full	23.9	0.001	0.421	0.001	0.088	5
	10000	24.1	0.006	0.48	0.004	0.194	5
	7000	23.9	0.007	0.48	0.005	0.207	5
4	Full	63.2	0.019	0.48	0.014	0.342	5
	50000	61.8	0.03	0.48	0.022	0.429	5
	5000	42	0.069	0.35	0.05	0.755	5
5	Full	79.6	0.031	0.48	0.023	0.439	5
	75000	78.2	0.043	0.48	0.032	0.518	5
	10000	50.4	0.074	0.323	0.054	0.818	5
	3000	33.6	0.109	0.225	0.077	1.172	5
6	Full	95.4	0.047	0.48	0.034	0.538	5
	50000	75.8	0.061	0.387	0.015	0.683	5
	30000	67.7	0.067	0.348	0.05	0.759	5
	5000	38.5	0.116	0.209	0.083	1.266	5
	2000	35.9	0.212	0.235	0.169	1.703	5
7	Full	95.2	0.058	0.412	0.042	0.641	5
	50000	74.4	0.072	0.326	0.053	0.81	5
	30000	66.5	0.081	0.292	0.059	0.904	5
	20000	59.6	0.089	0.264	0.066	1.002	5
	3000	31	0.168	0.145	0.12	1.825	5
	2000	26.9	0.193	0.128	0.135	2.063	5
8	Full	92.6	0.068	0.366	0.047	0.722	5
	30000	65.1	0.093	0.26	0.067	1.017	5
	20000	58.4	0.103	0.234	0.074	1.127	5
	10000	46.9	0.128	0.191	0.091	1.385	5
	3000	30	0.196	0.127	0.136	2.073	5
	1000	19.9	0.289	0.089	0.195	2.975	5

8.5 DISCUSSIONS OF RESULTS

8.5.1 Based on First Part of Analysis

1. From **Tables 8.3 to 8.10**, it is observed that barring the 1 storey frame, all the frames exhibit a peak value of moment in the top storey beam when subjected to lateral loads under semi rigid joint conditions.
2. It is generally observed that for the top storey beam, the moment developed due to lateral loads increases with increase in the joint rigidity, attain a peak value at a particular value of joint rigidity and then decreases with further increase in the joint stiffness till the frame joints become fully rigid. For all other stories, the beam moment increases monotonically with increase in joint rigidity.
3. It is also observed that as the number of storey increases, the peak moment in the top storey is observed at a higher value of joint rigidity.
4. For the two bay frames, the earthquake moments at the internal beam column joint of the top few storey also exhibit the phenomenon of peak moment under semi rigid joint conditions.
5. As the number of storey increases, the value of peak moment at the outer joint for the terrace level beam under earthquake loads remains almost constant. This is indicated in **Tables 8.11 and 8.13** for the single and double bay frames. The same observation holds good for the inner joint of a two bay frame as seen from **Table 8.15**.
6. From **Table 8.12** for single bay frames and **Table 8.14** for 2 bay frames, it is observed that as the number of storey increases, the ratio of the peak moment to fully rigid moment also increases. Also, the same is true for inner joint of the top storey in case of 2 bay frames as observed from **Table 8.16**.
7. **Tables 8.12, 8.14 and 8.16** also indicate that for an 8 storey frame, the ratio of peak moment to fully rigid moment is **2.46** for single bay and **2.31** for outer joint of 8 storey 2 bay frame, it is highest at **2.89**

for the inner joint of an 8 storey 2 bay frame.

8. It is also clear that although the peak moment is observed for the storey below the top storey, the ratio of peak moment to fully rigid moment remain near to 1 which indicates that the peak value at other levels below the terrace levels are not very significant. This is true for both the outer as well as the inner joint in case of 2 bay frames.

8.5.2 Based on Second Part of Analysis

1. From the study of deformed shape for all the frames, it is observed that the first hinge develops in the columns under lateral push.
2. The deformed shapes of all the frames indicates that for joints with lower value of rigidity, there are few plastic hinges which develop as compared to fully rigid frames. This shows that the structure with less rigidity behaves in a ductile manner.
3. It is observed from **Tables 8.17** and **8.18** that for single bay as well as for two bay frames, the effective damping at performance point in all the cases remains at 5% only indicating negligible damage in the frames under earthquake forces.
4. It is also observed from **Fig. 8.32** that for a single bay frames, there is hardly any difference in the performance points due to semi rigidity as compared to fully rigid joints for frames up to 3 storey. The same observation is valid for 2 bay frames also as seen in **Fig. 8.49**.
5. From the graphs of roof displacement versus base shear as shown in **Fig. 8.32** and **Fig. 8.49**, it can be seen that performance point for fully rigid frames is achieved at higher base shear and lower roof displacement for all the models indicating a better seismic performance. This trend points to the fact that in case the joints of an RC frame loses it's rigidity by the seismic vibrations, it's performance deteriorates.